Research Square

Preprints are preliminary reports that have not undergone peer review.
They should not be considered conclusive, used to inform clinical practice,
or referenced by the media as validated information.

Elucidating the Multi-Target Mechanisms of Niclosamide in Hepatocellular Carcinoma through Network Pharmacology, Molecular Docking, and Molecular Dynamics Simulations

Rushikesh Joshi
Poona College of Pharmacy
Satish Mandlik
Poona College of Pharmacy
Shrikant Nilewar
Maliba Pharmacy College, Uka Tarsadia University
Deepa Mandlik
deepa_ingawale@yahoo.com

Poona College of Pharmacy

Research Article

Keywords: Niclosamide, Hepatocellular carcinoma, In sillico, Network pharmacology, Molecular docking, Molecular dynamics simulation

Posted Date: April 1st, 2026

DOI: https://doi.org/10.21203/rs.3.rs-9148243/v1

License: This work is licensed under a Creative Commons Attribution 4.0 International License.
Read Full License

Additional Declarations: No competing interests reported.

Abstract

The Hepatocellular carcinoma (HCC) continues to be a major contributor to cancer-related deaths globally, fueled by intricate molecular diversity and widespread resistance to existing targeted treatments. Drug repurposing provides a strategy that is both effective and economical for identifying new therapeutic options. Niclosamide (NIC), which is approved by the food drug administration for use as an anthelmintic, has shown promise as a cancer treatment because it can affect multiple oncogenic signalling pathways. This study utilized an integrated in silico approach that combined network pharmacology, molecular docking, molecular dynamics (MD) simulations, and toxicity prediction to clarify the multitarget mechanisms of NIC in HCC. The analysis using network pharmacology found 252 overlapping targets between genes associated with NIC and those linked to HCC. The examination of protein–protein interactions underscored essential hub proteins such as AKT1 (Protein Kinase B alpha), Epidermal Growth Factor Receptor (EGFR), Proto-oncogene Tyrosine-Protein Kinase Src (SRC), Signal Transducer and Activator of Transcription 3 (STAT3), Janus Kinase 2 (JAK2), and Phosphoinositide-3-Kinase Regulatory Subunit 1 (PIK3R1). This indicates that NIC may play a role in vital oncogenic signalling networks. Analyses of Gene ontology (GO) and Kyoto *encyclopedia of genes and genomes* (KEGG) pathway enrichment showed a significant association with pathways such as Phosphoinositide 3-Kinase (PI3K)–AKT, ERBB, JAK–STAT, EGFR inhibitor resistance, and immune-related pathways. This highlights the polypharmacological nature of NIC. Molecular docking showed that NIC exhibits favorable binding affinities toward major hub targets, similar to those of the clinically used drug Sorafenib (SOR). Additionally, 100-ns MD simulations verified the dynamic stability and ongoing interactions of NIC with essential proteins like AKT, EGFR, and SRC, suggesting strong binding under physiological conditions. In silico toxicity assessment via the ProTox-III server indicated low to moderate toxicity levels, with hepatotoxicity considered acceptable and only minimal risks for mutagenicity or carcinogenicity. This extensive computational investigation endorses niclosamide as a multitarget, mechanistically sound, and relatively safe candidate for HCC therapy, thereby necessitating further experimental validation and formulation optimization.

1. Introduction

Hepatocellular carcinoma (HCC), which constitutes nearly 90% of primary liver cancer cases, is a significant global health issue due to its high rates of incidence and mortality. Recent estimates indicate that there are over 860,000 new cases and more than 750,000 deaths each year, with projections suggesting that the number of cases will surpass 1 million annually in the near future (Rumgay et al., 2022). HCC is one of the foremost contributors to cancer-related fatalities globally, as it is the sixth most frequently diagnosed cancer and the third most common cause of cancer deaths. The causes of HCC are numerous and closely linked to ongoing liver damage and chronic inflammation. Chronic infections with hepatitis B (HBV) and hepatitis C viruses are significant risk factors, as they facilitate the development of HCC through ongoing cycles of liver cell damage, regeneration, fibrosis, and cirrhosis (Bray et al., 2024). In many Asian and African regions, HBV continues to be the main cause, while in Western populations, metabolic dysfunction–associated steatotic liver disease and alcohol-related liver

disease are becoming more significant contributors to HCC. Other risk factors comprise exposure to aflatoxin, smoking, diabetes mellitus, and genetic or environmental conditions that contribute to ongoing liver damage (Amin et al., 2025). HCC typically arises in cirrhotic livers, accounting for about 80–90% of cases, underscoring the significant connection between chronic liver disease and malignant transformation. Its pathogenesis is fueled by chronic inflammation, fibrotic remodeling, genomic instability, and signalling pathways that are out of control, leading to unchecked cell proliferation, angiogenesis, and resistance to apoptosis. The prognosis for HCC continues to be unfavorable, even with improvements in treatment and surveillance. Surgical resection and liver transplantation are effective curative options only for early-stage disease, while locoregional and systemic therapies are used for more advanced stages but face limitations due to late diagnosis, underlying liver dysfunction, high recurrence rates, tumor heterogeneity, and therapeutic resistance (Lee, 2025).

Niclosamide (NIC) which is widely used to treat tapeworm infections, is a salicylanilide anthelmintic approved by the U.S. Food and Drug Administration. It has a long-established safety profile and is included in the World Health Organization's essential medicines list. Aside from its use as an antiparasitic drug, a wealth of preclinical studies has pointed to NIC potential as a repurposed anticancer agent (Y. Li et al., 2014). This promise stems from its ability to influence several signalling pathways that are key to tumor development such as Wnt/β-catenin, signal transducer and activator of transcription 3 (STAT3), nuclear factor kappa-light-chain-enhancer of activated B cells (NF-κB), mechanistic target of rapamycin (mTOR), and Notch as well as to disturb mitochondrial function and bring about apoptosis and cell cycle arrest in cancer cells (Z. Wang et al., 2022a). NIC has shown the ability to inhibit cancer cell proliferation, migration, and STAT3 signalling in HCC models, underscoring its potential usefulness in combating HCC progression and chemoresistance (Zhong et al., 2023).

Network-level strategies integrated with atomistic modelling create a robust computational pipeline for drug discovery and mechanism-of-action investigations: network pharmacology employs extensive databases and protein–protein interaction (PPI) analyses to pinpoint target sets and pathway enrichments pertinent to disease, directing the testing of compounds against specific proteins and pathways (Pinzi & Rastelli, 2019). Molecular docking predicts likely binding poses and relative affinities between small molecules and these prioritized targets, swiftly filtering candidates and creating testable hypotheses regarding binding modes; and molecular dynamics (MD) simulations provide further analysis by explicitly modelling atomic movements and solvent effects to evaluate the stability of docked complexes, conformational changes, and energetically plausible interactions over time (Shahzadi et al., 2024). These methods collectively diminish experimental burden, aid in elucidating polypharmacology and off-target effects, and enhance confidence in *in-silico* predictions when combined with suitable validation techniques (such as consensus scoring, ensemble docking, and adequately lengthy/replicated MD runs) (Jain et al., 2024).

The NIC has shown encouraging anticancer effects in HCC by inhibiting crucial oncogenic pathways like STAT3 and metabolic signalling, its low solubility in water and limited bioavailability pose major challenges for effective clinical application. Recent advances in translational and computational

research highlight the value of *in-silico* approaches such as network pharmacology, molecular docking, and MD simulations for thoroughly characterizing NIC target landscape and molecular interactions in HCC. These integrative strategies facilitate the identification of protein targets relevant to disease, the prediction of energetically favorable drug-target binding modes, and the evaluation of dynamic stability at atomic resolution. Together, they offer mechanistic insights that aid in experimental prioritization and the generation of therapeutic hypotheses. The successful application of advances in network pharmacology, along with docking and MD, to clarify complex compound–target interactions in cancer models highlights their usefulness for analysing NIC polypharmacology and enhancing its repurposing potential against HCC. This computational framework speeds up the assessment of candidates and improves the biological interpretability of NIC effects within a multi-pathway oncogenic context (Wang et al., 2022b).

2. Materials and Methods

2.1 Toxicity Analysis

The ProTox-III (https://tox.charite.de/protox3/) web server was used to forecast the toxicity profile of NIC (PubChem CID: 91,453). Oral toxicity, LD50, hepatotoxicity, carcinogenicity, and cytotoxicity were among the toxicity endpoints that were assessed once the molecule was submitted using its PubChem name. NIC probable safety and risk profile were revealed by classifying it into toxicity classes based on the forecasts (Banerjee et al., 2024a).

2.2 Network Pharmacology of active compound (NIC)

2.2.1 Identification of active compound (NIC)

All databases and software tools employed in this study can be accessed publicly. NIC canonical SMILES and chemical structure were obtained from the PubChem database (NIC, PubChem CID 4477; National Centre for Biotechnology Information, U.S. National Library of Medicine, PubChem) (https://pubchem.ncbi.nlm.nih.gov/compound/4477) (S. Kim et al., 2021). NIC Absorption, Distribution, Metabolism, and Excretion (ADME) attributes were assessed using an online tool to determine its drug-likeliness and pharmacokinetic profile (www.swissadme.ch) (Daina et al., 2017).

2.2.2 Prediction of NIC Target

The two-dimensional (2D) chemical structure of NIC obtained from pubchem, which was then sent to the Pharm Mapper server (http://www.lilab-ecust.cn/pharmmapper/) for target identification using reverse pharmacophore mapping (X. Wang et al., 2017). The Swiss Target Prediction platform (http://www.swisstargetprediction.ch/) which is limited to *Homo sapiens* and predicts targets based on chemical similarity and known ligand–protein interactions, was used in parallel to identify additional potential targets. Duplicate entries were eliminated when all targets obtained from Pharm Mapper, Swiss Target Prediction, and were integrated (S. Kim et al., 2023a).

2.2.3 Identification of HCC-associated genes

Using the search phrases "Hepatocellular Carcinoma", "HCC," and "liver cancer," HCC-related genes were found in Gene Cards (https://www.genecards.org/). To guarantee a strong illness relationship, only genes from the GeneCards database with a relevance score higher than 10 were kept. Using the UniProt database, all gathered targets were combined, duplicate entries were eliminated, and gene symbols were standardized (Bateman et al., 2023; Stelzer et al., 2016).

2.2.4 Identification of common targets (HCC- NIC)

Venny 2.1.0 was used to find the intersection of NIC-associated targets and HCC-related genes, about the overlapping genes considered potential therapeutic targets of NIC in relation to HCC (Arju Hossain et al., 2023).

2.2.5 compound target network construction

Topological analysis was conducted using Cytoscape software (v3.10.2) to identify the key hub genes within the PPI network. Using the Network Analyzer software, network topology features such as degree centrality, betweenness centrality, and closeness centrality were calculated to evaluate the significance of each node in the network. Hub genes were further identified using the CytoHubba plugin in Cytoscape, which ranked nodes based on degree centrality. The top ten genes with the highest degree values were selected as core targets and hub genes for additional molecular docking and MD simulation studies (Barabási & Oltvai, 2004; Doncheva et al., 2022). The intricate interaction between active compounds, filtrated targets, and pathways based on KEGG pathway enrichment analysis was reflected in a visual network created using Cytoscape software. This network illustrated the connections among active compounds, included targets, and primary pathways. Nodes represented the chemicals, pathways, and targets, while edges illustrated the interconnections among the pathways, targets, and other elements that could be utilized in NIC therapy for HCC. (Chen et al., 2021).

2.2.6 Protein-Protein Interaction Network

The PPI network was constructed by uploading the intersecting targets between NIC-associated genes and HCC related genes to the STRING database (https://string-db.org/) (Szklarczyk et al., 2021). The organism was limited to Homo sapiens, and a minimum interaction confidence score above 0.7 was established to guarantee high-confidence interactions. The resulting PPI network was imported into Cytoscape v3.10.2 for network analysis and visualization purposes (Khavari et al., 2025).

2.2.7 The enrichment analysis of the gene ontology (GO) and Kyoto Encyclopedia of Genes and Genomes (KEGG)\

Shiny GO v0.741 (http://bioinformatics.sdstate.edu/go74/) was used to do a functional enrichment analysis of the overlapping targets between genes linked to HCC and those linked to NIC. To clarify the key biological processes, molecular activities, and cellular localizations connected to NIC-mediated anticancer effects, GO analysis was performed across the three standard categories: biological process

(BP), cellular component (CC), and molecular function (MF). Processes pertaining to signal transduction, oxidative stress response, apoptosis, and cell proliferation regulation were primarily highlighted in the BP category. While the MF group focused on kinase activity, protein binding, adenosine triphosphate binding, and transcription factor binding all of which are essential for tumor development and survival the CC category (Ge et al., 2020) showed emphasis in cytoplasmic components, plasma membrane, nucleus, and protein complexes. To determine the major signalling pathways that NIC modulates in HCC, a KEGG pathway enrichment analysis was carried out concurrently. phosphatidylinositol 3-kinase–protein kinase B signalling pathway (PI3K-AKT), hypoxia-inducible factor 1 (HIF-1) signalling, apoptosis, cell cycle regulation, epidermal growth factor receptor (EGFR) signalling, wingless/integrated–β-catenin (Wnt/β-catenin) signalling pathway, and cancer pathways all known drivers of HCC progression, angiogenesis, metabolic reprogramming, and therapeutic resistance were primarily linked to the enriched pathways. These results confirm NIC's potential as a multi-target therapy agent in HCC by indicating that it may simultaneously modulate several carcinogenic pathways to produce its anti-HCC actions.

2.3. Molecular Docking Study

2.3.1. Preparation of Ligand and Protein

The SMILES structures of the selected NIC were provided by the PubChem database (S. Kim et al., 2023b). The purpose of the molecular docking research was to evaluate the NIC binding affinity and mechanisms of interaction with the identified hub proteins. The target proteins' three-dimensional (3D) structures were taken from the Protein Data Bank (PDB) (Hata et al., 2022). To find the lowest energy conformations appropriate for docking, the produced ligand structures were put through an energy reduction process using Avogadro software (Snyder & Kucukkal, 2021). The PDB provided the top target proteins' 3D crystal structures (Burley et al., 2022). Protein structures were processed using PyMOL to remove non-essential heteroatoms and crystallographic water molecules. Subsequently, the files for the ligand and protein were converted into PDBQT format with Kollman charges added to the proteins via AutoDock Tools, and polar hydrogens were included when necessary (Morris et al., 2009).

2.3.2. Docking arrangement and visualization

AutoDock Vina v1.2.5 was used for molecular docking using the default score and optimization settings (Eberhardt et al., 2021). To enable variable ligand binding, the docking grid box was centered on each protein's known or anticipated active site (Seeliger & De Groot, 2010a). All ligand-protein combinations were synthesized and docked using standard grid dimensions and exhaustiveness values to ensure consistency across targets (Forli et al., 2016a). The optimal docking poses were selected post-docking based on anticipated binding affinity and suitable binding within the active site (Seeliger & De Groot, 2010b). The docked complexes were viewed and analyzed using PyMOL v2.5 and BIOVIA Discovery Studio Visualizer to examine binding orientations and non-covalent interactions such as hydrogen π-π stacking, hydrophobic contacts, and bonding (Laskowski & Swindells, 2011).

2.4. Molecular Dynamics Simulation

The MD simulations were conducted with the DESMOND module of the Schrödinger Suite to verify the dynamic stability of the docked protein-ligand complexes. To establish the simulation, the protein-ligand complexes identified via molecular docking were brought into the Desmond system builder panel (Hernández-Rodríguez et al., 2020). During the development of the system, the solvent system was configured with the OPLS2004 force field. Each complex was placed in an explicit water environment using the TIP3P water model, within an orthorhombic simulation box that maintained a buffer distance of about 10 Å from the protein surface. After neutralising the system with suitable counterions (Na^+ and Cl^-), physiological ionic strength was maintained to replicate near-biological conditions. Following energy minimization, the complexes were equilibrated for 100 ps each to eliminate steric clashes and relax unfavorable interactions within the solvated system, using the constant number of particles, pressure, and temperature (NPT) ensemble prior to simulation. During the equilibration phase using NVT and NPT ensembles, a Nose-Hoover thermostat was used to control the temperature at 300 K, and a Martyna-Tobias-Klein barostat was applied to maintain the pressure at 1.01325 atm. The Particle Mesh Ewald (PME) method was utilized to calculate long-range electrostatic interactions at 2 fs time intervals, with a cutoff distance of 9 Å for short-range interactions. The production MD simulation was then performed at a constant temperature of 300 K and pressure of 1.01325 atm for a duration of 100 ns. An analysis of the trajectory produced in the simulation was conducted to examine the stability and behavior of the protein-ligand complexes under dynamic conditions. The analysis following the simulation encompassed an assessment of the root mean square deviation (RMSD), root mean square fluctuation (RMSF), secondary structure elements (SSE), protein–ligand interaction profiles (comprising hydrogen bonds, hydrophobic contacts, ionic interactions, and water bridges), and ligand characteristics (including rGyr, solvent accessible surface area (SASA), molecular surface area (MolSA), and polar surface area (PSA) (L. Li et al., 2024).

3. Results

3.1 Toxicity analysis

The ProTox-III web server was used to predict the toxicity profile of NIC. The analysis of the radar plot showed that NIC has low to moderate toxicity probabilities for most of the assessed endpoints. The compound exhibited low predicted levels of cytotoxicity, mutagenicity, and carcinogenicity; however, predictions indicated moderate levels of hepatotoxicity and acute oral toxicity. The likelihood of organ-specific toxicities, such as cardiotoxicity, nephrotoxicity, neurotoxicity, and respiratory toxicity, stayed within acceptable limits. Moreover, NIC showed moderate interactions with certain cytochrome P450 isoforms, indicating a controllable metabolic liability. In general, the anticipated toxicity profile indicates a positive safety–risk balance, warranting further exploration of NIC in anticancer drug repurposing studies. The predicted toxicity profile of NIC was visualized using a radar plot generated by the ProTox-III web server (Fig. 1).

3.2 Network Pharmacology Results

3.2.1 Compound Screening and Drug- Likeness Evaluation of NIC

The physicochemical properties and chemical structure of NIC were sourced from the PubChem database, after which they were assessed for drug-likeness via Lipinski's Rule of Five and subjected to ADME analysis using Swiss ADME. With an adequate molecular weight and hydrogen-bonding properties, NIC was found to mostly meet Lipinski's requirements. However, its low water solubility and relatively high lipophilicity may have an impact on oral bioavailability. The physicochemical properties of NIC shown in Table 1 were predicted using the Swiss ADME. Although these drawbacks, NIC's proven pharmacological action and promise for repurposing in cancer treatment made it appropriate for additional molecular docking and dynamics modelling research. Table.1 shows Physicochemical properties of NIC based on Lipinski’s rule of five

3.2.2 Drug- Disease common target

A total of 12,281 genes linked to HCC were identified from the Gene Cards database after filtering by relevance score and eliminating duplicates. After target normalization, the analysis of NIC through Swiss Target Prediction yielded 278 putative drug targets. Venn diagram analysis, illustrated in Fig. 2, revealed 252 overlapping targets between NIC-associated targets and HCC-related genes. These were considered candidate therapeutic targets for further network pharmacology and molecular docking analyses.

3.2.3 The PPI Network Construction and Identification of Potential Hub Genes in NIC Associated with HCC

The overlapping targets of NIC and HCC were submitted to the STRING database to establish a PPI network. The resulting network, shown in Fig. 3A, displayed a highly interconnected structure that indicated strong functional connections among the candidate therapeutic targets. The extensive edge distribution and dense clustering suggest that these proteins might be coordinated participants in biological processes associated with HCC. Key hub genes were identified through topological analysis of the PPI network, using centrality parameters. The hub genes with the highest ranks were AKT serine/threonine kinase 1 (AKT1), epidermal growth factor receptor (EGFR), proto-oncogene tyrosine-protein kinase Src (SRC), STAT3, phosphatidylinositol-4,5-bisphosphate 3-kinase catalytic subunit alpha (PIK3CA), heat shock protein 90 alpha family class A member 1 (HSP90AA1), phosphoinositide-3-kinase regulatory subunit 1 (PIK3R1), protein tyrosine kinase 2 (focal adhesion kinase 1) (PTK2), and signal transducer and activator of transcription 1 (STAT1). These hub nodes, as shown in Fig. 3B, demonstrated high degree values, underscoring their central regulatory functions within the NIC–HCC interaction network and indicating their potential significance as therapeutic targets. This core network highlights how these targets serve as integrative components in oncogenic signalling pathways that are pertinent to HCC progression. To clarify the connection between HCC and the recognized candidate targets, a disease–target interaction network was created.. The PPI network's top 10 hub genes are listed in Table 2.

Table 2
Top 10 hub genes from the PPI network

Sr. no	Full form	Gene name	Degree	Betweenness centrality	Closeness centrality
1	Protein Kinase B (AKT Serine/Threonine Kinase)	AKT1	58	0.109	0.475
2	Epidermal Growth Factor Receptor	EGFR	52	0.085	0.459
3	Heat Shock Protein 90 Alpha Family Class A Member 1	HSP90AA1	50	0.106	0.462
4	Janus Kinase 2	JAK2	23	0.003	0.386
5	Phosphatidylinositol-4,5-Bisphosphate 3-Kinase Catalytic Subunit Alpha	PIK3CA	34	0.012	0.394
6	Phosphatidylinositol-4,5-Bisphosphate 3-Kinase Regulatory Subunit 1	PIK3R1	36	0.021	0.406
7	Protein Tyrosine Kinase 2 (Focal Adhesion Kinase, FAK)	PTK2	21	0.003	0.381
8	SRC Proto-Oncogene, Non-Receptor Tyrosine Kinase	SRC	48	0.028	0.436
9	Signal Transducer and Activator of Transcription 3	STAT3	49	0.049	0.454
10	Signal Transducer and Activator of Transcription 1	STAT1	30	0.013	0.421

3.2.4 Target–Disease Interaction Network of Hepatocellular Carcinoma

To identify potential genes associated with HCC, a target–disease interaction network was constructed. The network illustrates the connection between HCC and its associated disease-related molecular targets. As shown in Fig. 4, multiple genes are linked to HCC, indicating that hepatocarcinogenesis is regulated by a complex network of interacting proteins. The dense interconnections among these targets highlight the multifactorial nature of HCC progression and emphasize the involvement of several signalling pathways responsible for cell proliferation, apoptosis, inflammation, and tumor development. This network offers a detailed depiction of the molecular landscape of HCC and acts as a basis for pinpointing possible therapeutic targets for additional study.

3.2.5 Niclosamide–Target–Hepatocellular Carcinoma Interaction Network

A drug–target–disease interaction network was integrated and constructed to investigate the potential therapeutic mechanisms of NIC against HCC. The network depicts the connections among NIC, its anticipated molecular targets, and genes linked to HCC. As shown in Fig. 5, NIC interacts with several protein targets that are also implicated in HCC pathogenesis, suggesting a multi-target pharmacological mechanism. The intricate network structure emphasizes the complicated regulatory connections linking drug targets with disease-related genes, suggesting that NIC may perform its anticancer function by modulating multiple signaling pathways implicated in tumor growth, survival, and metastasis. The results offer a systems-level insight into the possible molecular mechanisms through which NIC might have therapeutic effects in HCC.

3.2.6 GO and KEGG Enrichment Analysis Result

ShinyGO was used to conduct the GO and KEGG enrichment analyses with a significance threshold of $P < 0.05$. The top 10 enriched terms in each category were chosen based on fold enrichment and false discovery rate (FDR) values. Gene Ontology (GO) analysis indicated that the enriched biological processes (BP) were predominantly linked to the regulation of intracellular signalling, especially receptor tyrosine kinase–mediated pathways like the ERBB signalling pathway, ERBB2 receptor signalling, and the PI3K signalling pathway. Additional enrichment was observed in processes related to inositol lipid–mediated signalling and peptide hormone response, indicating that the identified targets are largely involved in growth factor–dependent proliferative and survival signalling mechanisms relevant to HCC. In terms of cellular components (CC), the enriched targets were primarily localized in membrane-associated signalling complexes, including cell junction structures, extrinsic components of the plasma membrane, and phosphatidylinositol 3-kinase complexes (class IA and class I), suggesting their role in receptor activation, signal transduction, and intercellular communication. The analysis of molecular function (MF) revealed a significant enrichment in activities related to kinases, such as transmembrane receptor protein tyrosine kinase activity, protein kinase activity, kinase binding, and protein phosphatase binding. This underscores the significance of phosphorylation-dependent oncogenic signaling pathways. Furthermore, KEGG pathway enrichment analysis identified several cancer-related pathways, including EGFR tyrosine kinase inhibitor resistance, PD-L1 expression and the PD-1 checkpoint pathway in cancer, the JAK–STAT signalling pathway, the prolactin signalling pathway, and Hepatitis B infection. These findings collectively indicate that the overlapping NIC–HCC targets are involved in key oncogenic, immunological, and viral-associated hepatocarcinogenesis pathways, providing mechanistic insight into the potential therapeutic role of NIC in HCC (Zheng et al., 2025). The top enriched GO terms and KEGG pathways NIC–HCC targets are illustrated in Fig. 6.

3.3 Molecular Docking Results of NIC and sorafenib (SOR) binding affinity against HCC associated hub target

To confirm the binding affinity of NIC and SOR against 09 HCC-associated hub targets, molecular docking analysis was conducted. To assess the binding affinity of NIC and SOR with the selected hub targets related to HCC, a molecular docking analysis was conducted.. The binding energies obtained from docking simulations demonstrated varying affinities of both ligands toward the target proteins. NIC

exhibited the strongest binding affinity with AKT (− 10 kcal/mol), followed by SRC (− 9.5 kcal/mol), EGFR (− 8.6 kcal/mol), PTK2 (− 8.5 kcal/mol), PIK3CA (− 8.2 kcal/mol), JAK2 and PIK3R1 (− 8.0 kcal/mol), HSP90AA1 (− 7.5 kcal/mol), and STAT3 (− 6.2 kcal/mol). In comparison, SOR demonstrated the highest binding affinity toward AKT (− 12.5 kcal/mol) and SRC (− 11.2 kcal/mol), followed by PTK2 (− 9.4 kcal/mol), PIK3R1 (− 9.0 kcal/mol), EGFR and PIK3CA (− 8.6 and − 8.2 kcal/mol respectively), JAK2 (− 8.0 kcal/mol), HSP90AA1 (− 7.5 kcal/mol), and STAT3 (− 7.4 kcal/mol). Overall, both ligands demonstrated favorable binding interactions with key oncogenic targets involved in HCC-related signalling pathways, with AKT and SRC showing comparatively stronger binding affinities. As shown in Table 3, all binding energies were negative, indicating favourable interactions. The 2D and 3D binding interactions of NIC with key hub proteins implicated in HCC shown in Fig. 7 and the SOR key hub proteins implicated in HCC shown in Fig. 8.

Table no. 3 Table showing top 09 targets their binding affinity with SOR and NIC

Sr.no	Full form	Target	Ligands	
			NIC (kcal/mol)	SOR (kcal/mol)
1	Protein Kinase B (AKT Serine/Threonine Kinase)	AKT	-10	-12.5
2	Epidermal Growth Factor Receptor	EGFR	-8.6	-8.6
3	Heat Shock Protein 90 Alpha Family Class A Member 1	HSP90AA1	-7.5	-7.5
4	Janus Kinase 2	JAK2	-8.0	-8.0
5	Phosphatidylinositol-4,5-Bisphosphate 3-Kinase Catalytic Subunit Alpha	PIK3CA	-8.2	-8.2
6	Phosphatidylinositol-4,5-Bisphosphate 3-Kinase Regulatory Subunit 1	PIK3R1	-8.0	-9.0
7	Protein Tyrosine Kinase 2 (Focal Adhesion Kinase, FAK)	PTK2	-8.5	-9.4
8	SRC Proto-Oncogene, Non-Receptor Tyrosine Kinase	SRC	-9.5	-11.2
9	Signal Transducer and Activator of Transcription 3	STAT 3	-6.2	-7.4

3.4 Molecular Dynamics Simulation Results

The conformational behaviour and dynamic stability of the top-ranked NIC-protein complexes identified through molecular docking investigations were examined using MD simulations. By using atomic movements that are reliant on time, Protein-ligand interactions may be investigated in nearly

physiological conditions this is MD simulations, which circumvent the static limitations of molecular docking.

3.4.1 Comparative MD *Analysis of NIC–AKT and* SOR *–AKT Complexes*

Over a 100 ns trajectory, comparative MD simulation analysis of the AKT1–NIC and AKT1–sorafenib complexes demonstrated stable binding behavior, with significant variations in dynamic stability and interaction patterns (Figs. 9 and 10). The RMSD profile of the AKT1–NIC complex (Fig. 9A) revealed a gradual stabilization of the system throughout the simulation. The protein backbone RMSD varied between roughly 4.5 and 5.8 Å, while the ligand RMSD was relatively constant at around ~ 2.8 to 3.5 Å, indicating that the ligand was stably accommodated within the AKT1 binding pocket. The RMSF analysis (Fig. 9B) indicated that most residues had fluctuations under 2 Å, with slightly increased flexibility noted primarily in loop regions. The mapping of protein–ligand interactions (Fig. 9C) demonstrated that NIC established stable connections with essential residues such as TRP80, VAL271, TYR272, ARG273, ASP274, and ASP292 via hydrogen bonds, hydrophobic interactions, and water-mediated bridges. The interaction fraction plot (Fig. 9D) provided additional confirmation of persistent contacts, especially with TRP80 (~ 98%), VAL271 (~ 87%), TYR272, and ASP292 (~ 76%). The AKT1–NIC complex retained about 40.94% of its total secondary structure during the simulation, with 19.08% α-helices and 21.86% β-strands, as indicated by secondary structure element (SSE) analysis (Fig. 9E). This suggests that ligand binding did not significantly disrupt the protein architecture. The evaluation of ligand properties (Fig. 9F) revealed a low ligand RMSD of approximately 0.3–0.5 Å following equilibration, a compact radius of gyration of around 4.0 Å, and the presence of intermittent intramolecular hydrogen bonds. These findings suggest that the ligand conformation within the binding pocket is relatively rigid and stable. When compared to others, the AKT1–SOR complex (Fig. 10A) showed greater initial fluctuations in the simulation's early phase before reaching stability, with the protein RMSD settling around ~ 3.0–3.5 Å and the ligand RMSD varying between ~ 3.0–4.0 Å. The RMSF analysis (Fig. 10B) showed relatively higher residue fluctuations, especially around residues 90–120 and near residue ~ 300, suggesting increased local flexibility of the protein structure. The interaction analysis (Fig. 10C) revealed that sorafenib primarily interacted with residues like TRP80, ILE84, VAL270, TYR272, ASP292, and GLU298 through hydrophobic contacts and water-mediated interactions. The analysis of the interaction fraction (Fig. 10D) revealed a lower persistence of interactions, with significant contacts including TRP80, LEU264, ASP292 (~ 53%), GLU298 (~ 57%), and ILE84. The assessment of secondary structure (Fig. 10E) revealed a structural content of about 43.59%, comprising 20.55% α-helices and 23.04% β-strands, indicating that the overall protein folding was maintained during the simulation. Further analysis of ligand properties (Fig. 10F) indicated a higher RMSD for the ligand (~ 1.5–1.8 Å), a larger radius of gyration (~ 6.3–6.8 Å), and the lack of intramolecular hydrogen bonds, implying that sorafenib exhibits relatively greater conformational flexibility within the binding site.

3.4.2 Comparative MD *Analysis of NIC–EGFR and* SOR *– EGFR Complexes*

Molecular dynamics (MD) simulations were conducted to assess the stability and interaction dynamics of the EGFR–ligand complexes over a 100 ns trajectory under NPT conditions at 300 K (Figs. 11 and 12). The EGFR–niclosamide complex (Fig. 11A) demonstrated a highly stable RMSD profile throughout the simulation, with the protein backbone RMSD stabilizing around ~ 2.0 2.4 Å and the ligand RMSD closely following the protein trajectory, indicating a well-stabilized ligand orientation within the binding site. The RMSF analysis (Fig. 11B) indicated that fluctuations were relatively low for most residues, generally staying below 2 Å. This suggests that the protein maintained overall structural stability during the simulation. The interaction diagram of the protein and ligand (Fig. 11C) showed that niclosamide established stabilizing connections with several key residues, such as PHE856, LYS745, LEU788, and ASP855, via hydrogen bonds and hydrophobic contacts. The interaction fraction plot (Fig. 11D) validated the presence of strong and enduring contacts, especially with ASP855 and PHE856, along with further interactions involving LYS745 and LEU747. The assessment of secondary structure (Fig. 11E) showed that the EGFR protein maintained stable secondary structural elements throughout the simulation, with around 30.52% α-helix and 15.36% β-strand content, leading to a total composition of about 45.88%. This indicates that ligand binding did not significantly disrupt the overall protein structure. The analysis of ligand properties (see Fig. 11F) provided additional evidence of stable ligand conformational parameters, such as a consistent radius of gyration, molecular surface area, solvent accessible surface area, and polar surface area values. At the same time, occasional intramolecular hydrogen bonds suggested slight conformational adjustments that did not destabilize the ligand structure.

For the EGFR–sorafenib complex (Fig. 12A), the RMSD profile showed greater fluctuations during the initial ~ 15 ns, followed by stabilization of the system. The protein backbone RMSD equilibrated around ~ 2.8–3.2 Å, while the ligand RMSD fluctuated near ~ 3.5–4.5 Å, indicating that the complex achieved structural equilibrium after early conformational adjustments. The analysis of RMSF (Fig. 12B) indicated that the majority of residues displayed fluctuations under 2 Å, while slightly greater flexibility was noted in loop regions and around residues approximately at positions 100 and 300, which are generally linked to flexible segments of the protein. The mapping of protein–ligand interactions (see Fig. 12C) showed that sorafenib engaged with several crucial residues such as TRP80, LEU264, ILE84, ASP292, and GLU298 via hydrogen bonds, hydrophobic interactions, and water-mediated connections. The interaction fraction plot (Fig. 12D) further demonstrated ongoing contacts, especially with ASP292 and GLU298, as well as hydrophobic interactions involving residues like LEU264 and TRP80. The analysis of secondary structure (Fig. 12E) demonstrated that EGFR kept stable secondary structural elements throughout the simulation, suggesting that the protein's global architecture was preserved. The analysis of ligand properties (Fig. 12F) showed that the values for ligand RMSD, radius of gyration, molecular surface area, solvent accessible surface area, and polar surface area remained relatively stable. Furthermore, the absence of intramolecular hydrogen bonds indicates that sorafenib exhibits moderate conformational flexibility within the binding pocket.

3.4.3 Comparative MD Analysis of NIC and SOR in Complex with SRC

We performed molecular dynamics (MD) simulations to investigate the stability and dynamic behavior of SRC–ligand complexes over a 100 ns trajectory at 300 K under NPT conditions (Figs. 13 and 14). In the SRC–SOR complex (Fig. 13A), the RMSD profile displayed moderate fluctuations during the simulation's initial phase, followed by a gradual stabilization of the system. The protein backbone RMSD varied around ~ 2.2–2.8 Å, suggesting that the SRC structure achieved equilibrium and remained stable during the trajectory. The RMSD of the ligand was relatively lower, usually varying around ~ 0.8–1.6 Å, indicating that sorafenib kept a stable orientation in the SRC binding pocket. The RMSF analysis (Fig. 13B) showed that the majority of residues had fluctuations under 2 Å, which confirms the overall stability of the protein. However, slightly greater flexibility was noted in the loop regions, especially around residue indices close to ~ 150 and ~ 250. Protein–ligand interaction mapping (Fig. 13C) revealed that sorafenib interacted with several key residues, including ILE297, LYS298, MET317, VAL326, LEU328, ILE339, TYR343, MET344, SER345, GLY347, ASN394, LEU396, ALA406, ASP407, PHE408, and LEU410 via hydrogen bonding, hydrophobic interactions, and water-mediated bridges. The interaction fraction analysis (Fig. 13D) revealed that persistent contacts involve residues like ILE297, LEU396, and PHE408. Analysis of secondary structure elements (SSE) (Fig. 13E) revealed that the SRC protein maintained stable secondary structural components, consisting of approximately 28.68% α-helix and 13.79% β-strand, resulting in a total SSE composition of about 42.47%. This indicates that the binding of SOR did not significantly disturb the overall structure of the protein. The examination of ligand characteristics (Fig. 13F) showed stable conformational parameters such as the radius of gyration, molecular surface area, solvent accessible surface area, and polar surface area. Additionally, no intramolecular hydrogen bonds were observed during the simulation. In contrast, the SRC–NIC complex (Fig. 14A) demonstrated a stable RMSD trajectory during the simulation, with the protein backbone RMSD oscillating within ~ 2.3–2.9 Å and the ligand RMSD consistently lower, indicating that NIC was stably accommodated within the SRC binding site. The RMSF analysis (Fig. 14B) revealed that the majority of residues exhibited fluctuations under 2 Å, with slightly heightened flexibility noted around loop regions, especially near residues ~ 150 and ~ 250. The mapping of protein–ligand interactions (Fig. 14C) showed that NIC interacts strongly with key SRC residues such as LYS298, VAL326, ASP407, and PHE408 via hydrogen bonding and hydrophobic interactions. The interaction fraction plot (Fig. 14D) further validated the presence of strong and enduring contacts with residues like LYS298 (~ 49%), VAL326 (~ 98%), PHE408 (~ 98%), and ASP407 (~ 92%), suggesting that the ligand binds stably within the catalytic pocket. The SRC protein maintained stable secondary structural elements, with around 26.50% α-helix and 14.47% β-strand content, resulting in a total SSE composition of approximately 40.97%. This indicates that ligand binding preserved the protein's structural integrity (Fig. 14E). The evaluation of the ligand characteristics (see Fig. 14F) indicated that conformational parameters like the radius of gyration, molecular surface area, solvent accessible surface area, and polar surface area remained stable. However, occasional intramolecular hydrogen bonds were noted, indicating slight conformational adjustments that did not compromise ligand stability.

4. Discussion

Hepatocellular carcinoma remains one of the most prevalent primary liver malignancies and continues to contribute substantially to global cancer-related mortality. Despite improvements in systemic therapies, the clinical outcomes for patients with advanced HCC remain unsatisfactory due to tumor heterogeneity, late diagnosis, and the development of resistance to available targeted therapies such as SOR. These limitations emphasize the need to explore alternative therapeutic strategies capable of modulating multiple molecular pathways involved in hepatocarcinogenesis. Drug repurposing has emerged as a promising strategy in this regard because it enables the identification of new therapeutic applications for already approved drugs with known safety profiles (Qi et al., 2025).

Niclosamide, a widely recognized anthelmintic medication, has recently attracted considerable interest for its possible anticancer effects via drug repurposing approaches. Increasing evidence suggests that NIC exerts wide-ranging antitumor effects through the modulation of various oncogenic signaling pathways associated with cancer cell proliferation, survival, and metastasis. Mechanistically, NIC has been demonstrated to inhibit several crucial signaling pathways including STAT3, PI3K/AKT, Wnt/β-catenin, NF-κB, and mTOR, which are frequently dysregulated in HCC (Z. Wang et al., 2022c). In addition to its direct effects on tumor cells, niclosamide has shown the ability to interfere with the preservation of cancer stem cells and signaling driven by the tumor microenvironment. This results in a reduction of tumor growth and advancement. Recent research indicates that niclosamide can induce apoptosis, inhibit cell proliferation, and disrupt mitochondrial oxidative phosphorylation in cancer cells, underscoring its multi-target therapeutic potential (Laila et al., 2025). Because of its pharmacological properties, niclosamide is a promising candidate for repurposing in cancer treatment, especially for complex malignancies like HCC that involve multiple signaling pathways in disease progression. This study utilized an integrated computational framework that combines network pharmacology, MD, MD simulation, and toxicity prediction to investigate the potential mechanisms by which NIC may have therapeutic effects on HCC. In addition to efficacy, the safety profile of a potential therapeutic agent is an important consideration. Therefore, an *in-silico* toxicity prediction using the ProTox-III platform was conducted. The results suggested that NIC exhibits low to moderate toxicity, with acceptable hepatotoxicity levels and minimal risks related to mutagenicity or carcinogenicity. These findings align with the long-standing clinical use of NIC as an antiparasitic drug and further support its potential suitability for repurposing in cancer therapy (Banerjee et al., 2024b).

Network pharmacology analysis revealed 252 overlapping targets between NIC-associated genes and genes implicated in HCC. This overlap suggests that niclosamide may exert its pharmacological activity through a broad and interconnected network of molecular interactions rather than a single target. Such multi-target characteristics are particularly relevant for complex diseases like cancer, where multiple signalling pathways contribute simultaneously to tumor initiation, progression, and metastasis (Aslam et al., 2024).

Further investigation through PPI network analysis identified several highly connected nodes that may play central roles in the NIC–HCC interaction network. The top ten hub genes identified were AKT1, EGFR, SRC, STAT3, PIK3CA, HSP90AA1, PIK3R1, PTK2, and STAT1, JAK 2. These proteins represent critical regulators of cellular signalling pathways associated with tumor growth, proliferation, survival, and metastasis. For example, AKT1 serves as a crucial element of the PI3K/AKT pathway, which fosters cell survival and metabolic regulation and is often disrupted in liver cancer (Zhu et al., 2022). EGFR signalling is known to stimulate tumor cell proliferation and angiogenesis, while SRC, a non-receptor tyrosine kinase, contributes to tumor invasion and metastatic progression. Similarly, transcription factors such as STAT3 and STAT1 are involved in cytokine signalling and immune regulation, which are essential components of the tumor microenvironment (Jin et al., 2022; Ploeger et al., 2022; Song et al., 2022).

Other identified hub genes further highlight the complexity of the regulatory network associated with HCC. PIK3CA and PIK3R1 represent catalytic and regulatory subunits of phosphoinositide 3-kinase, a central pathway involved in oncogenic signalling (Fruman et al., 2017). PTK2, also known as focal adhesion kinase, is closely associated with cell migration and metastasis, while HSP90AA1 functions as a molecular chaperone that stabilizes many oncogenic proteins ss(Huang et al., 2021; Y. Kim et al., 2025). The identification of these hub genes suggests that NIC may influence multiple signalling cascades simultaneously, thereby potentially disrupting key mechanisms responsible for HCC progression.

In order to gain a better understanding of the biological significance of these targets, a GO enrichment analysis was performed. The analysis showed that the overlapping targets were mainly associated with biological processes (BPs) like intracellular signaling regulation, oxidative stress response, apoptosis, and cell proliferation regulation. These biological processes are essential for tumor development and survival. As for cellular localization, the enriched targets were predominantly linked to membrane-related structures such as plasma membrane complexes and cell junction components, highlighting their involvement in receptor-mediated signal transduction. The analysis of molecular function underscored the enrichment of activities related to kinases, such as protein kinase activity, transmembrane receptor tyrosine kinase activity, and kinase binding. These results underscore the pivotal function of phosphorylation-dependent signalling processes in the development of HCC (Lin et al., 2022).

Complementary KEGG pathway enrichment analysis further indicated that the overlapping targets are involved in multiple cancer-related signaling pathways. The pathways that were enriched to a significant degree included the PI3K–AKT signalling pathway, EGFR signalling pathway, JAK–STAT signalling pathway, ERBB signalling pathway, and PD-1/PD-L1 immune checkpoint pathway. Additional enrichment was observed in pathways associated with HIF-1 signalling, apoptosis regulation, cell cycle control, and HBV infection, all of which are known contributors to hepatocarcinogenesis. These results suggest that NIC may exert therapeutic effects by simultaneously regulating multiple oncogenic and immune-related pathways involved in HCC pathogenesis (Kanehisa et al., 2023).

Molecular docking analysis was conducted to confirm the possible interactions between NIC and the identified hub targets, and the results were compared with those of SOR, a drug used clinically for HCC. The docking results demonstrated that NIC displayed favorable binding affinities toward several key oncogenic proteins. The strongest binding interaction was observed with AKT, showing a binding energy of approximately − 10 kcal/mol, followed by SRC (− 9.5 kcal/mol), EGFR (− 8.6 kcal/mol), PTK2 (− 8.5 kcal/mol), and PIK3CA (− 8.2 kcal/mol). Additional interactions were observed with JAK2 and PIK3R1 (− 8.0 kcal/mol), HSP90AA1 (− 7.5 kcal/mol), and STAT3 (− 6.2 kcal/mol). These negative binding energy values indicate thermodynamically favorable interactions between NIC and the target proteins. Although SOR generally demonstrated slightly stronger binding affinities for certain targets, NIC exhibited comparable interaction patterns with several key proteins, particularly AKT and SRC, suggesting its potential to modulate major oncogenic pathways involved in HCC (Forli et al., 2016b).

To further confirm the stability of the docked complexes and evaluate the dynamic behavior of protein–ligand interactions, MD simulations were performed on the top-ranked complexes identified via molecular docking. MD simulations yield a time-resolved depiction of protein–ligand interactions under near-physiological conditions, enabling the assessment of conformational stability and interaction persistence over time. This study involved 100-ns MD simulations of niclosamide complexes with essential hub proteins such as AKT, EGFR, and SRC. The results were compared to those from the clinically used HCC drug Sorafenib to establish a benchmark for binding stability and interaction dynamics.

The MD simulation of the AKT–niclosamide complex over a 100 ns trajectory showed that protein–ligand interactions were stable. According to the RMSD profile, while the ligand RMSD was fairly constant which suggested that niclosamide kept a stable orientation in the binding pocket the backbone of AKT gradually stabilized after equilibration. The RMSF analysis showed minimal residue fluctuations, with the majority of residues demonstrating deviations under 2 Å, apart from slightly flexible loop regions. Key residues like TRP80, VAL271, TYR272, ARG273, and ASP292 exhibited persistent interactions via hydrogen bonding and hydrophobic contacts. Analysis of the secondary structure confirmed that the overall architecture of the protein remained stable during the simulation. The results imply that niclosamide creates a dynamically stable complex with AKT, bolstering its possible function in modulating the PI3K/AKT signaling pathway related to the progression of HCC.

During the 100 ns simulation, the EGFR–niclosamide complex demonstrated a stable dynamic behavior. The RMSD analysis showed that throughout the simulation, both the protein backbone and ligand reached equilibrium and maintained stable trajectories. The RMSF results indicated low residue fluctuations, especially in the ligand-binding region, which suggests stable interactions within the catalytic pocket. According to interaction analysis, niclosamide established stable connections with several important residues, such as PHE723, LYS745, LEU747, ILE759, MET766, ASP855, and PHE856 via hydrogen bonding and hydrophobic interactions. Assessment of secondary structure indicated that the EGFR protein maintained its structural integrity while binding to the ligand. The results indicate that

niclosamide can have a stable interaction with EGFR and may disrupt EGFR-mediated signaling pathways linked to the progression of HCC.

The MD simulation of the SRC–NIC complex showed that it maintained stable conformational behavior during the entire simulation period. The RMSD profile showed that the SRC backbone quickly attained equilibrium and exhibited stable deviations for the rest of the trajectory. Residue fluctuation analysis demonstrated that the majority of residues displayed low RMSF values, thereby confirming overall structural stability. Stable interactions of niclosamide with key residues like LYS298, VAL326, ASP407, and PHE408 were established via hydrogen bonding and hydrophobic contacts. Analysis of the secondary structure additionally showed that the SRC protein's overall folding was maintained throughout the simulation. These observations imply that NIC sustains a stable attachment within the SRC catalytic pocket and may influence SRC-mediated oncogenic signalling pathways associated with tumor invasion and metastasis.

In summary, the findings of this comprehensive computational analysis indicate that NIC could function as a multi-target therapeutic agent that modulates various key molecular pathways implicated in hepatocellular carcinoma. NIC may interfere with interconnected signaling networks that promote tumor growth, survival, and metastasis by simultaneously affecting hub proteins such as AKT1, EGFR, SRC, STAT3, PIK3CA, JAK2, HSP90AA1, PIK3R1, PTK2, and STAT1. A comprehensive systems-level perspective on the potential mechanisms underlying NIC anti-HCC activity is provided by the combination of network pharmacology, docking analysis, and MD simulations.

While the current study offers useful insights into mechanisms, it is crucial to recognize that its results are mainly derived from computational methods. To validate the predicted interactions and assess the therapeutic efficacy of NIC in HCC models, additional experimental studies both *in vitro* and *in vivo* are required. Future studies might concentrate on refining methods for delivering drugs or creating NIC-based derivatives that have enhanced pharmacokinetic properties.

Conclusion

Considering the complex molecular landscape of HCC and the high costs and time requirements associated with traditional experimental drug discovery methods, computational strategies like network pharmacology combined with molecular docking and MD simulations provide an effective framework for identifying potential therapeutic candidates. This research employed a thorough in silico approach to explore NIC multitarget therapeutic potential for HCC. Analysis using network pharmacology indicated that niclosamide might influence several major oncogenic targets, including AKT1, EGFR, SRC, STAT3, PIK3CA, and JAK2. This regulation occurs via essential signaling pathways like PI3K–AKT, JAK–STAT, ERBB, and EGFR-related pathways that are recognized for their roles in tumor proliferation, angiogenesis, metastasis, and survival in HCC. Further support for the findings came from later molecular docking and molecular dynamics simulations. These demonstrated that niclosamide establishes stable and energetically advantageous interactions with multiple hub proteins, particularly AKT, EGFR, and SRC. The

dynamic stability observed in MD simulations indicates that niclosamide can consistently bind within the catalytic pockets of these oncogenic targets under physiological conditions. The results underscore niclosamide's potential to concurrently modulate various signaling pathways implicated in hepatocarcinogenesis, bolstering the case for its repurposing as a promising multitarget therapeutic candidate for HCC. Although these findings are promising, the current study has some limitations. findings derive mainly from computational analyses, and HCC is a disease characterized by high heterogeneity due to the interplay of intricate molecular and clinical factors. As a result, the anticipated interactions and mechanisms need to be further confirmed using experimental methods. Future research should aim to validate these findings using suitable *in vitro* and *in vivo* models, as well as investigate optimized drug delivery strategies to address the pharmacokinetic limitations of niclosamide. In summary, this research offers a thorough computational perspective on the possible mechanisms of NIC in HCC and serves as a basis for additional experimental and translational studies.

Declarations

Consent for publication

Not applicable.

Competing interests

The authors declared no conflicts of interest.

Conflict of interest

We have no conflict of interest.

Funding

No funding was received for this research work.

Author Contribution

RJ and SN has performed the experimental parts. SM was responsible for literature research and drafting of a manuscript. DM has critically revised the manuscript. All authors have read and approved the manuscript.

Acknowledgement

We want to thank you, Dr. A. P. Pawar, Principal, Poona College of Pharmacy, Bharati Vidyapeeth (Deemed to be University), for providing the necessary facilities to carry out this research work.

Data Availability

All data and materials are available upon request.

References

1. Amin N, Anwar J, Sulaiman A, Naumova NN, Anwar N (2025) Hepatocellular Carcinoma: A Comprehensive Review. Dis (Basel Switzerland) 13(7). https://doi.org/10.3390/diseases13070207
2. Arju Hossain M, Sohel M, Rahman MH, Hasan MI, Sharif Khan M, Al Amin M, Islam Z, M., Peng S (2023) Bioinformatics and In silico approaches to identify novel biomarkers and key pathways for cancers that are linked to the progression of female infertility: A comprehensive approach for drug discovery. PLoS ONE 18(1):e0265746. https://doi.org/10.1371/journal.pone.0265746
3. Aslam S, Qasim M, Noor F, Shahid M, Ashfaq UA, Munir S, Al-Harthi HF, Mashraqi MM, Waqas U, Khurshid M (2024) Potential Target Metabolites From Gut Microbiota Against Hepatocellular Carcinoma: A Network Pharmacology and Molecular Docking Study. Int J Microbiol 2024(1). https://doi.org/10.1155/2024/4286228
4. Banerjee P, Kemmler E, Dunkel M, Preissner R (2024a) ProTox 3.0: a webserver for the prediction of toxicity of chemicals. Nucleic Acids Res 52(W1):W513–W520. https://doi.org/10.1093/NAR/GKAE303
5. Banerjee P, Kemmler E, Dunkel M, Preissner R (2024b) ProTox 3.0: a webserver for the prediction of toxicity of chemicals. Nucleic Acids Res 52(W1):W513–W520. https://doi.org/10.1093/nar/gkae303
6. Barabási AL, Oltvai ZN (2004) Network biology: understanding the cell's functional organization. Nat Rev Genet 5(2):101–113. https://doi.org/10.1038/nrg1272
7. Bateman A, Martin MJ, Orchard S, Magrane M, Ahmad S, Alpi E, Bowler-Barnett EH, Britto R, Bye-A-Jee H, Cukura A, Denny P, Dogan T, Ebenezer TG, Fan J, Garmiri P, da Gonzales C, Hatton-Ellis LJ, Hussein E, Ignatchenko A, Zhang A, J (2023) UniProt: the Universal Protein Knowledgebase in 2023. Nucleic Acids Res 51(D1):D523–D531. https://doi.org/10.1093/nar/gkac1052
8. Bray F, Laversanne M, Sung H, Ferlay J, Siegel RL, Soerjomataram I, Jemal A (2024) Global cancer statistics 2022: GLOBOCAN estimates of incidence and mortality worldwide for 36 cancers in 185 countries. Cancer J Clin 74(3):229–263. https://doi.org/10.3322/caac.21834
9. Burley SK, Berman HM, Duarte JM, Feng Z, Flatt JW, Hudson BP, Lowe R, Peisach E, Piehl DW, Rose Y, Sali A, Sekharan M, Shao C, Vallat B, Voigt M, Westbrook JD, Young JY, Zardecki C (2022) Protein Data Bank: A Comprehensive Review of 3D Structure Holdings and Worldwide Utilization by Researchers, Educators, and Students. Biomolecules 12(10):1425. https://doi.org/10.3390/biom12101425

10. Chen X, Xu M, An Y (2021) Identifying the essential nodes in network pharmacology based on multilayer network combined with random walk algorithm. *Journal of Biomedical Informatics*, *114*. https://doi.org/10.1016/j.jbi.2020.103666
11. Daina A, Michielin O, Zoete V (2017) SwissADME: A free web tool to evaluate pharmacokinetics, drug-likeness and medicinal chemistry friendliness of small molecules. *Scientific Reports*, *7*. https://doi.org/10.1038/srep42717
12. Doncheva NT, Morris JH, Holze H, Kirsch R, Nastou KC, Cuesta-Astroz Y, Rattei T, Szklarczyk D, von Mering C, Jensen LJ (2022) Cytoscape stringApp 2.0: Analysis and Visualization of Heterogeneous Biological Networks. J Proteome Res 22(2):637–646. https://doi.org/10.1021/acs.jproteome.2c00651
13. Eberhardt J, Santos-Martins D, Tillack AF, Forli S (2021) AutoDock Vina 1.2.0: New Docking Methods, Expanded Force Field, and Python Bindings. J Chem Inf Model 61(8):3891–3898. https://doi.org/10.1021/acs.jcim.1c00203
14. Forli S, Huey R, Pique ME, Sanner MF, Goodsell DS, Olson AJ (2016a) Computational protein–ligand docking and virtual drug screening with the AutoDock suite. Nat Protocols 2016 11:5(5):905–919. https://doi.org/10.1038/nprot.2016.051. *11*
15. Forli S, Huey R, Pique ME, Sanner MF, Goodsell DS, Olson AJ (2016b) Computational protein-ligand docking and virtual drug screening with the AutoDock suite. Nat Protoc 11(5):905–919. https://doi.org/10.1038/nprot.2016.051
16. Fruman DA, Chiu H, Hopkins BD, Bagrodia S, Cantley LC, Abraham RT (2017) The PI3K Pathway in Human Disease. Cell 170(4):605–635. https://doi.org/10.1016/j.cell.2017.07.029
17. Ge SX, Jung D, Jung D, Yao R (2020) ShinyGO: a graphical gene-set enrichment tool for animals and plants. Bioinformatics 36(8):2628–2629. https://doi.org/10.1093/bioinformatics/btz931
18. Hata K, Kobayashi N, Sugimura K, Qin W, Haxholli D, Chiba Y, Yoshimi S, Hayashi G, Onoda H, Ikegami T, Mulholland CB, Nishiyama A, Nakanishi M, Leonhardt H, Konuma T, Arita K (2022) Structural basis for the unique multifaceted interaction of DPPA3 with the UHRF1 PHD finger. Nucleic Acids Res 50(21):12527–12542. https://doi.org/10.1093/nar/gkac1082
19. Hernández-Rodríguez M, Mendoza Sánchez PI, Macías Perez ME, Cruz ER, Jiménez EM, Aceves-Hernández JM, Nicolás-Vázquez MI, Ruvalcaba RM (2020) In vitro and computational studies of natural products related to perezone as anti-neoplastic agents. *Biochimie*, *171–172*, 158–169. https://doi.org/10.1016/j.biochi.2020.03.003
20. Huang D, Savage SR, Calinawan AP, Lin C, Zhang B, Wang P, Starr TK, Birrer MJ, Paulovich AG (2021) A highly annotated database of genes associated with platinum resistance in cancer. Oncogene 2021 40(46):6395–6405. https://doi.org/10.1038/s41388-021-02055-2. *40*
21. Jain NK, Tailang M, Chandrasekaran B, Khazaleh N, Thangavel N, Makeen HA, Albratty M, Najmi A, Alhazmi HA, Zoghebi K, Alagusundaram M, Jain HK (2024) Integrating network pharmacology with molecular docking to rationalize the ethnomedicinal use of Alchornea laxiflora (Benth.) Pax & K.

Hoffm. for efficient treatment of depression. *Frontiers in Pharmacology*, *15*. https://doi.org/10.3389/fphar.2024.1290398

22. Jin A, Zhang C, Zheng W, Xian J, Yang W, Liu T, Chen W, Li T, Wang B, Pan B, Li Q, Cheng J, Wang P, Hu B, Zhou J, Fan J, Yang X, Guo W (2022) CD155/SRC complex promotes hepatocellular carcinoma progression via inhibiting the p38 MAPK signalling pathway and correlates with poor prognosis. Clin Translational Med 12(4):e794. https://doi.org/10.1002/ctm2.794
23. Kanehisa M, Furumichi M, Sato Y, Kawashima M, Ishiguro-Watanabe M (2023) KEGG for taxonomy-based analysis of pathways and genomes. Nucleic Acids Res 51(D1):D587–D592. https://doi.org/10.1093/nar/gkac963
24. Khavari F, Najafi R, Afshar S, Jalali A, Hashemi M, Soltanian A, Nouri F (2025) A network-based analysis to identify a piRNA-target signature related to colorectal cancer prognosis: in silico and in vitro study. Discover Oncol 16(1):590. https://doi.org/10.1007/s12672-025-02373-x
25. Kim S, Chen J, Cheng T, Gindulyte A, He J, He S, Li Q, Shoemaker BA, Thiessen PA, Yu B, Zaslavsky L, Zhang J, Bolton EE (2021) PubChem in 2021: new data content and improved web interfaces. Nucleic Acids Res 49(D1):D1388–D1395. https://doi.org/10.1093/nar/gkaa971
26. Kim S, Chen J, Cheng T, Gindulyte A, He J, He S, Li Q, Shoemaker BA, Thiessen PA, Yu B, Zaslavsky L, Zhang J, Bolton EE (2023a) PubChem 2023 update. Nucleic Acids Res 51(D1):D1373–D1380. https://doi.org/10.1093/nar/gkac956
27. Kim S, Chen J, Cheng T, Gindulyte A, He J, He S, Li Q, Shoemaker BA, Thiessen PA, Yu B, Zaslavsky L, Zhang J, Bolton EE (2023b) PubChem 2023 update. Nucleic Acids Res 51(D1):D1373–D1380. https://doi.org/10.1093/nar/gkac956
28. Kim Y, Lim SY, Kim HO, Ha SJ, Park JA, Won YW, Chae S, Lim KS (2025) Combination Strategies with HSP90 Inhibitors in Cancer Therapy: Mechanisms, Challenges, and Future Perspectives. Pharmaceuticals 2025 18(8):1083. https://doi.org/10.3390/ph18081083. *18*
29. Laila UE, Zhao Zlong, Xu DY, Liu H, Xu ZX (2025) Pharmacological advances and therapeutic applications of niclosamide in cancer and other diseases. Eur J Med Chem 290(4):117527. https://doi.org/10.1016/j.ejmech.2025.117527
30. Laskowski RA, Swindells MB (2011) LigPlot+: Multiple Ligand–Protein Interaction Diagrams for Drug Discovery. J Chem Inf Model 51(10):2778–2786. https://doi.org/10.1021/ci200227u
31. Lee MH (2025) Public health strategies for hepatocellular carcinoma: from risk factors to prevention and control. J Liver Cancer 25(2):204–216. https://doi.org/10.17998/jlc.2025.07.25
32. Li L, Mohammed AH, Auda NA, Alsallameh SMS, Albekairi NA, Muhseen ZT, Butch CJ (2024) Network Pharmacology, Molecular Docking, and Molecular Dynamics Simulation Analysis Reveal Insights into the Molecular Mechanism of Cordia myxa in the Treatment of Liver Cancer. Biology 13(5). https://doi.org/10.3390/biology13050315
33. Li Y, Li PK, Roberts MJ, Arend RC, Samant RS, Buchsbaum DJ (2014) Multi-targeted therapy of cancer by niclosamide: A new application for an old drug. Cancer Lett 349(1):8–14. https://doi.org/10.1016/j.canlet.2014.04.003

34. Lin Y, He Z, Gao X, Lu L, Lu C, Huang J, Luo M, Ye J, Liang R (2022) Integrative Analysis Reveals the Potential Role and Prognostic Value of GOLM1 in Hepatocellular Carcinoma. *Oxidative Medicine and Cellular Longevity*, *2022*. https://doi.org/10.1155/2022/8284500
35. Morris GM, Ruth H, Lindstrom W, Sanner MF, Belew RK, Goodsell DS, Olson AJ (2009) AutoDock4 and AutoDockTools4: Automated Docking with Selective Receptor Flexibility. J Comput Chem 30(16):2785. https://doi.org/10.1002/jcc.21256
36. Pinzi L, Rastelli G (2019) Molecular Docking: Shifting Paradigms in Drug Discovery. Int J Mol Sci 20(18). https://doi.org/10.3390/ijms20184331
37. Ploeger C, Schreck J, Huth T, Fraas A, Albrecht T, Charbel A, Ji J, Singer S, Breuhahn K, Pusch S, Köhler BC, Springfeld C, Schirmacher P, Mehrabi A, Goeppert B, Roessler S (2022) STAT1 and STAT3 Exhibit a Crosstalk and Are Associated with Increased Inflammation in Hepatocellular Carcinoma. Cancers 14(5):1154. https://doi.org/10.3390/cancers14051154
38. Qi D, Qin Y, Zhu H, Li Y, Han S (2025) Resistance of first-line targeted drugs in hepatocellular carcinoma: the epigenetic regulation mechanisms. Cell Death Disease 2025 16:1(1):875. https://doi.org/10.1038/s41419-025-08105-x. *16*
39. Rumgay H, Arnold M, Ferlay J, Lesi O, Cabasag CJ, Vignat J, Laversanne M, McGlynn KA, Soerjomataram I (2022) Global burden of primary liver cancer in 2020 and predictions to 2040. J Hepatol 77(6):1598–1606. https://doi.org/10.1016/j.jhep.2022.08.021
40. Seeliger D, De Groot BL (2010a) Ligand docking and binding site analysis with PyMOL and Autodock/Vina. J Comput Aided Mol Des 24(5):417–422. https://doi.org/10.1007/s10822-010-9352-6
41. Seeliger D, De Groot BL (2010b) Ligand docking and binding site analysis with PyMOL and Autodock/Vina. J Comput Aided Mol Des 24(5):417–422. https://doi.org/10.1007/s10822-010-9352-6
42. Shahzadi Z, Yousaf Z, Anjum I, Bilal M, Yasin H, Aftab A, Booker A, Ullah R, Bari A (2024) Network pharmacology and molecular docking: combined computational approaches to explore the antihypertensive potential of Fabaceae species. Bioresources Bioprocess 11(1). https://doi.org/10.1186/s40643-024-00764-6
43. Snyder HD, Kucukkal TG (2021) Computational Chemistry Activities with Avogadro and ORCA. J Chem Educ 98(4):1335–1341. https://doi.org/10.1021/acs.jchemed.0c00959
44. Song S, Yu Z, You Y, Liu C, Xie X, Lv H, Xiao F, Zhu Q, Qin C (2022) EGFR/MET promotes hepatocellular carcinoma metastasis by stabilizing tumor cells and resisting to RTKs inhibitors in circulating tumor microemboli. Cell Death Disease 2022 13(4):351. https://doi.org/10.1038/s41419-022-04796-8. *13*
45. Stelzer G, Rosen N, Plaschkes I, Zimmerman S, Twik M, Fishilevich S, Iny Stein T, Nudel R, Lieder I, Mazor Y, Kaplan S, Dahary D, Warshawsky D, Guan-Golan Y, Kohn A, Rappaport N, Safran M, Lancet D (2016) The GeneCards Suite: From Gene Data Mining to Disease Genome Sequence Analyses. Curr Protocols Bioinf 54(1301–). https://doi.org/10.1002/cpbi.5

46. Szklarczyk D, Gable AL, Nastou KC, Lyon D, Kirsch R, Pyysalo S, Doncheva NT, Legeay M, Fang T, Bork P, Jensen LJ, von Mering C (2021) The STRING database in 2021: customizable protein-protein networks, and functional characterization of user-uploaded gene/measurement sets. Nucleic Acids Res 49(D1):D605–D612. https://doi.org/10.1093/nar/gkaa1074
47. Wang X, Shen Y, Wang S, Li S, Zhang W, Liu X, Lai L, Pei J, Li H (2017) PharmMapper 2017 update: a web server for potential drug target identification with a comprehensive target pharmacophore database. Nucleic Acids Res 45(W1):W356–W360. https://doi.org/10.1093/nar/gkx374
48. Wang Z, Ren J, Du J, Wang H, Liu J, Wang G (2022a) Niclosamide as a Promising Therapeutic Player in Human Cancer and Other Diseases. Int J Mol Sci 23(24). https://doi.org/10.3390/ijms232416116
49. Wang Z, Ren J, Du J, Wang H, Liu J, Wang G (2022b) Niclosamide as a Promising Therapeutic Player in Human Cancer and Other Diseases. Int J Mol Sci 23(24). https://doi.org/10.3390/ijms232416116
50. Zhong X, Fan XG, Chen R (2023) Repurposing Niclosamide as a Therapeutic Drug against Acute Liver Failure by Suppressing Ferroptosis. Pharmaceutics 15(7). https://doi.org/10.3390/pharmaceutics15071950
51. Zhu Q, Yu Y, Zhang Y, Wang X (2022) VLCAD inhibits the proliferation and invasion of hepatocellular cancer cells through regulating PI3K/AKT axis. Clin Translational Oncol 2021 24:5(5):864–874. https://doi.org/10.1007/s12094-021-02733-3. *24*

Figures

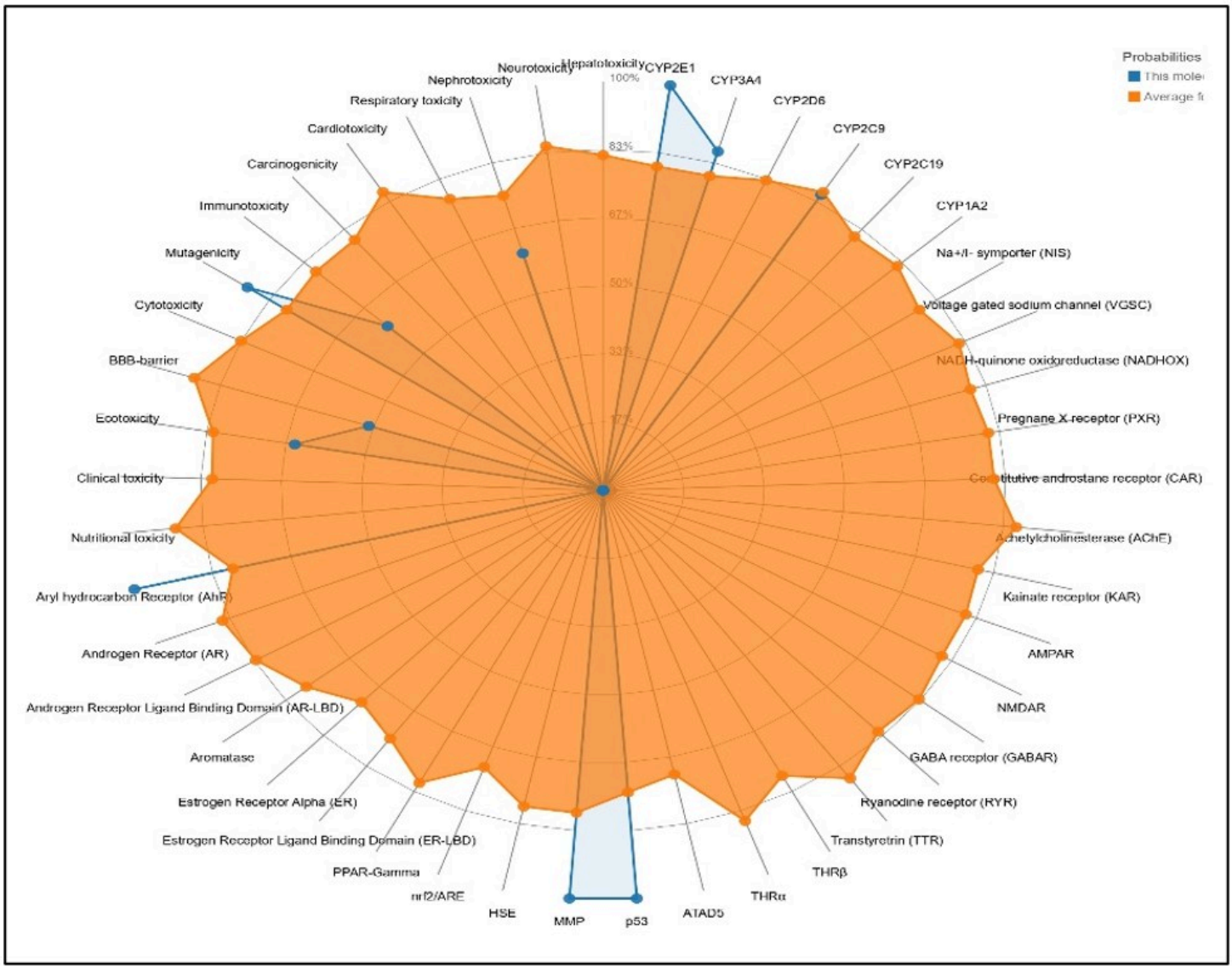

Figure 1

In silico toxicity profile of NIC predicted using the ProTox-III web server.

The radar plot illustrates predicted probabilities for major toxicity endpoints and metabolic interactions. The blue trace denotes NIC, while the orange area represents the average reference profile, indicating overall low to moderate predicted toxicity and a favorable *in silico* safety profile.

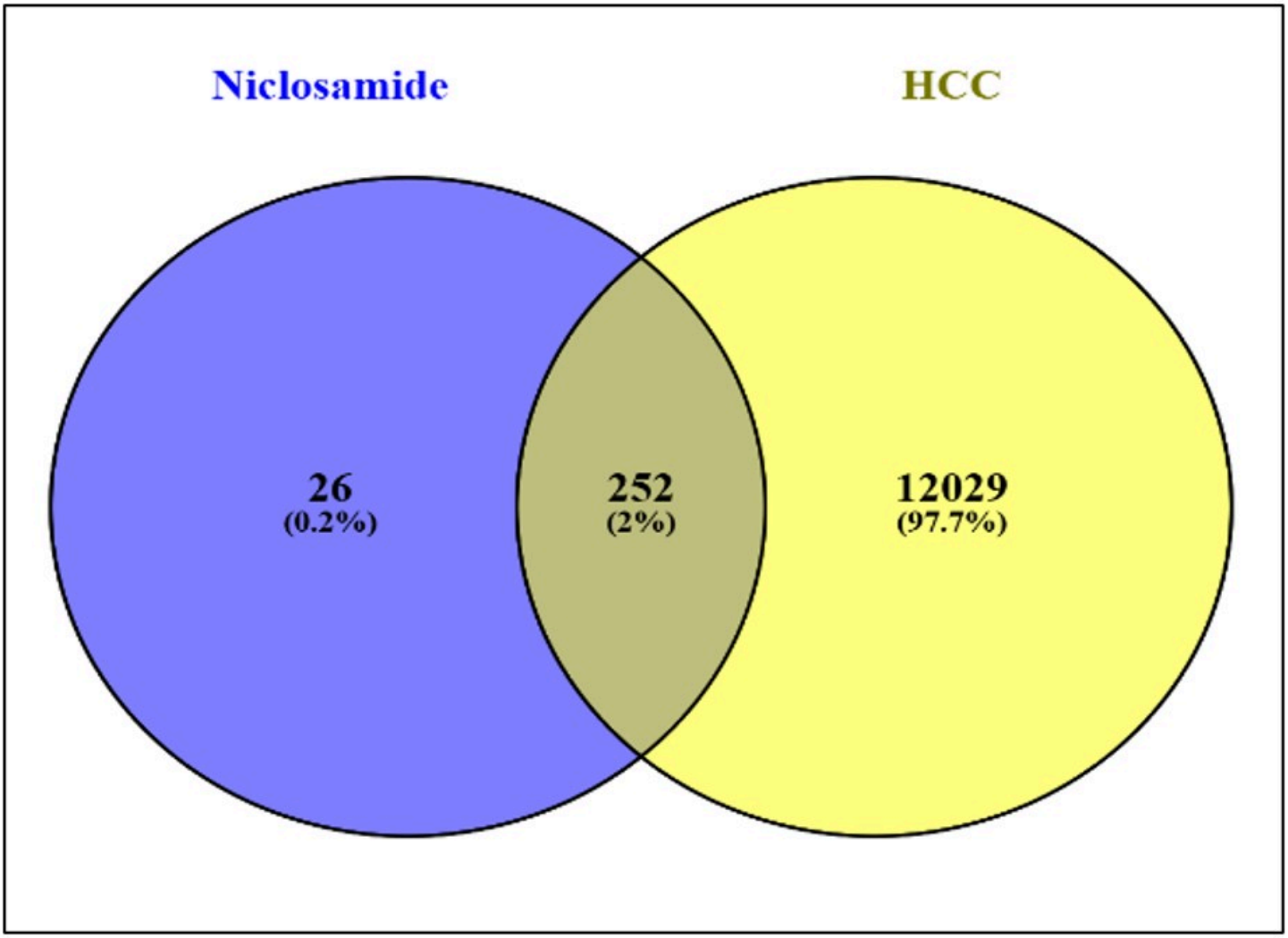

Figure 2

Venn diagram illustrating the possible therapeutic target of NIC for HCC treatment

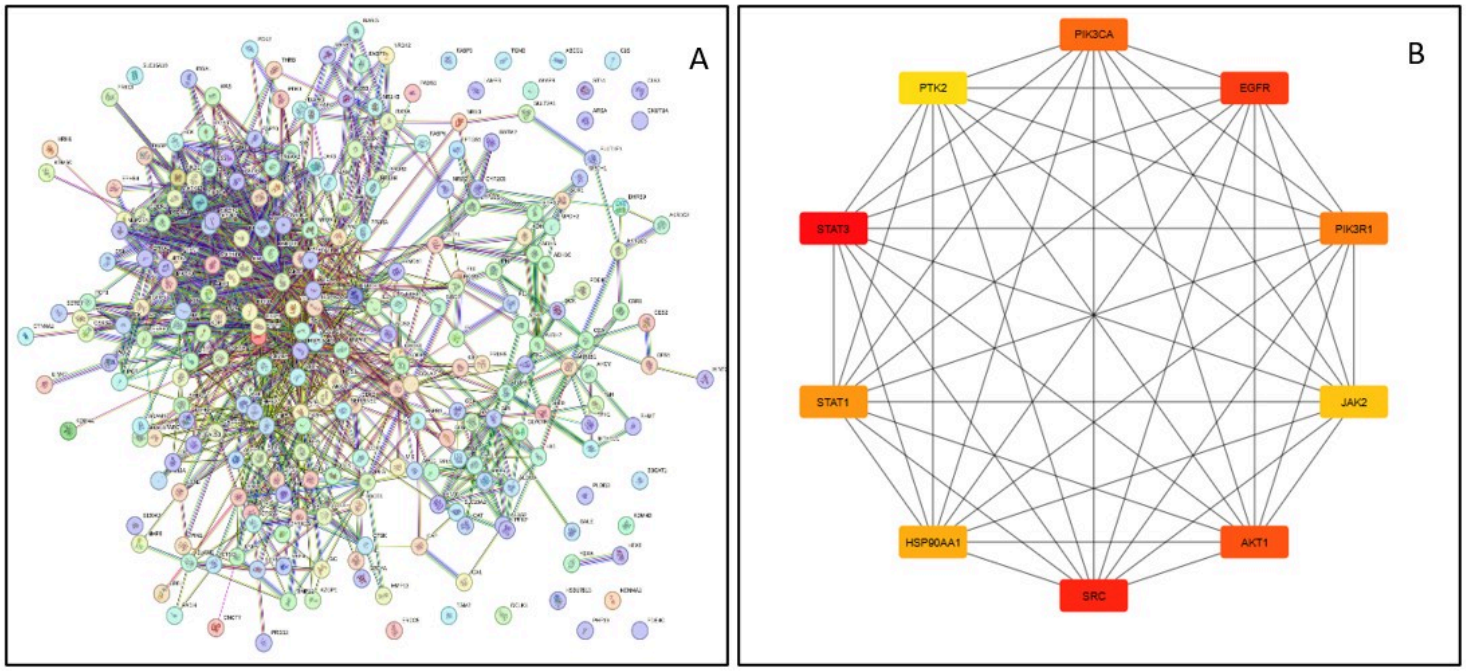

Figure 3

Network pharmacology analysis of NIC-associated targets in HCC

(A) Protein–protein interaction (PPI) network of overlapping NIC–HCC targets showing extensive functional connectivity.
(B) Hub gene interaction network highlighting the top-ranked targets based on topological analysis.

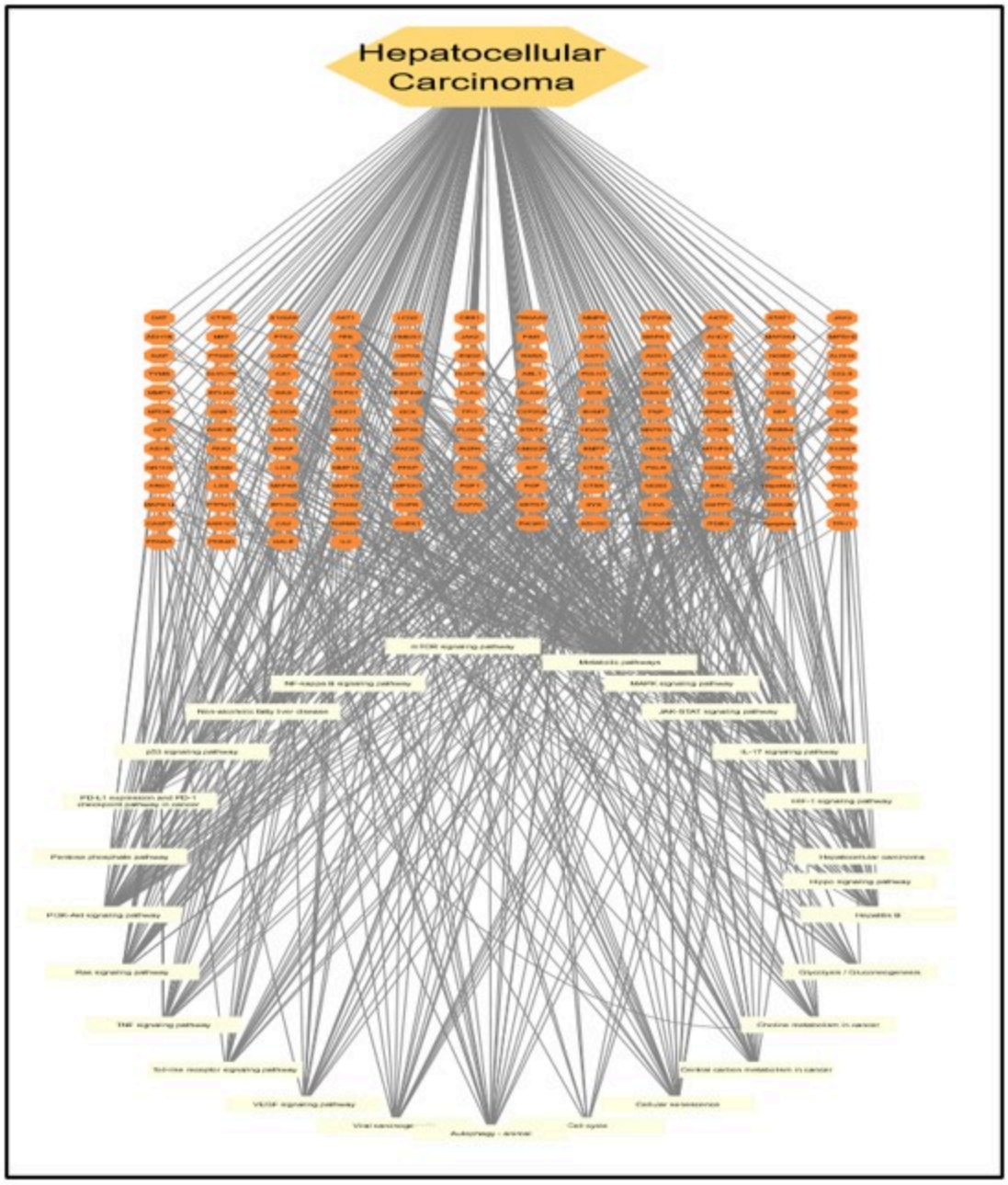

Figure 4

Disease–target network demonstrating the multi-target regulatory potential of NIC in HCC.

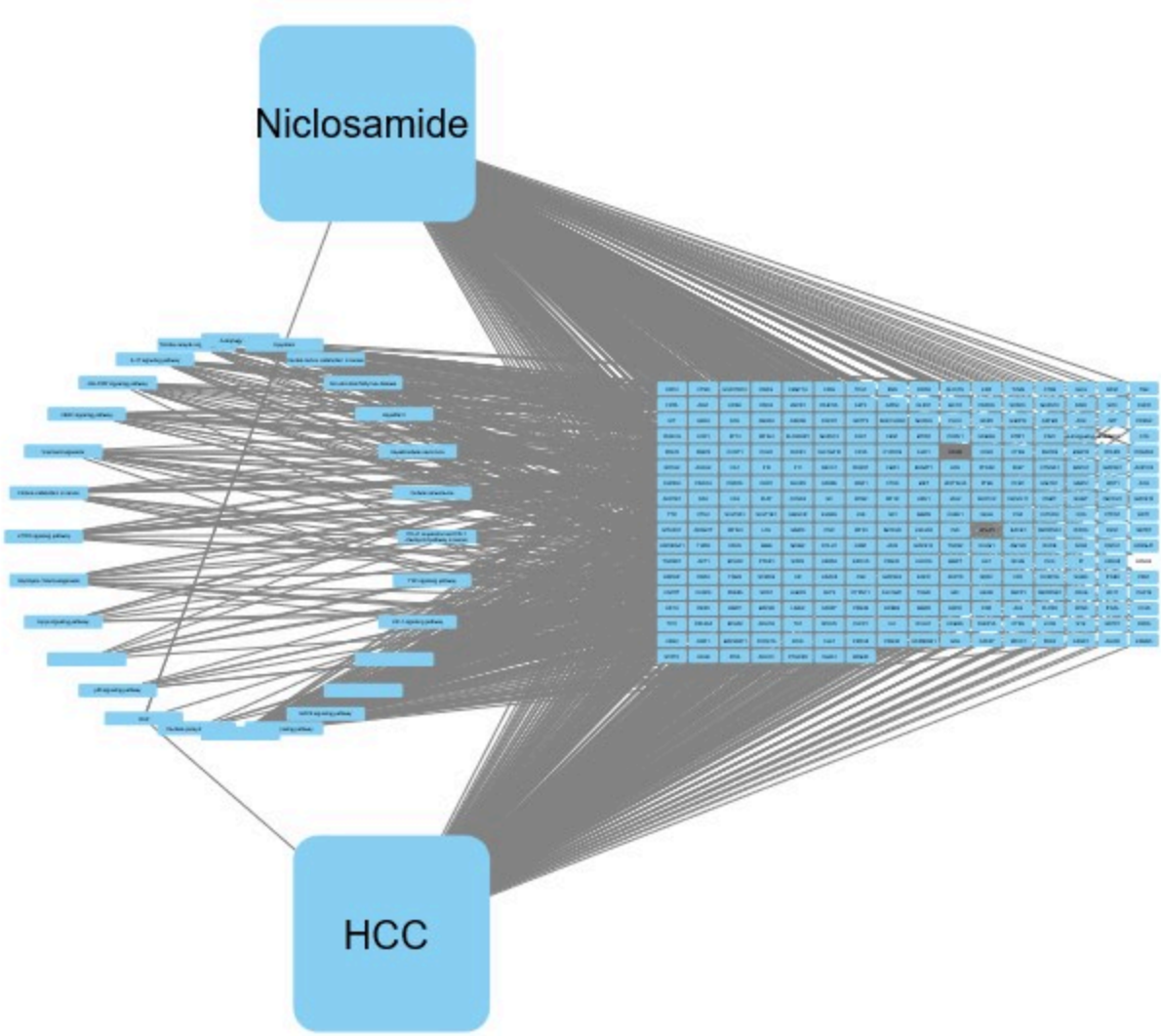

Figure 5

Niclosamide–Target–HCC interaction network.

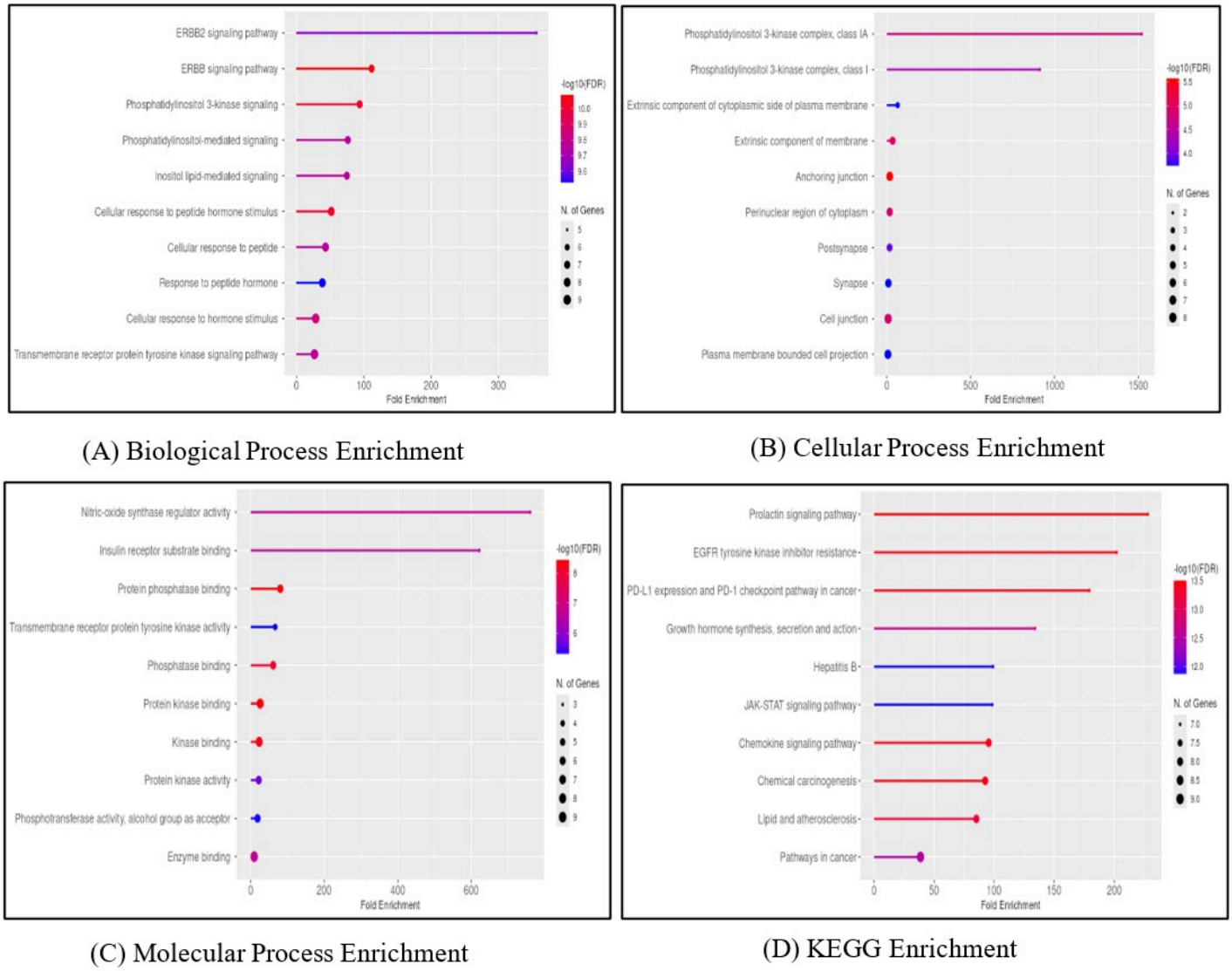

Figure 6

GO and KEGG enrichment analysis of overlapping targets.

(A) Biological process, (B) Cellular component, (C) Molecular function, (D) KEGG pathway enrichment. The x-axis represents fold enrichment; circle size indicates gene count and colour scale represents -log10 (FDR).

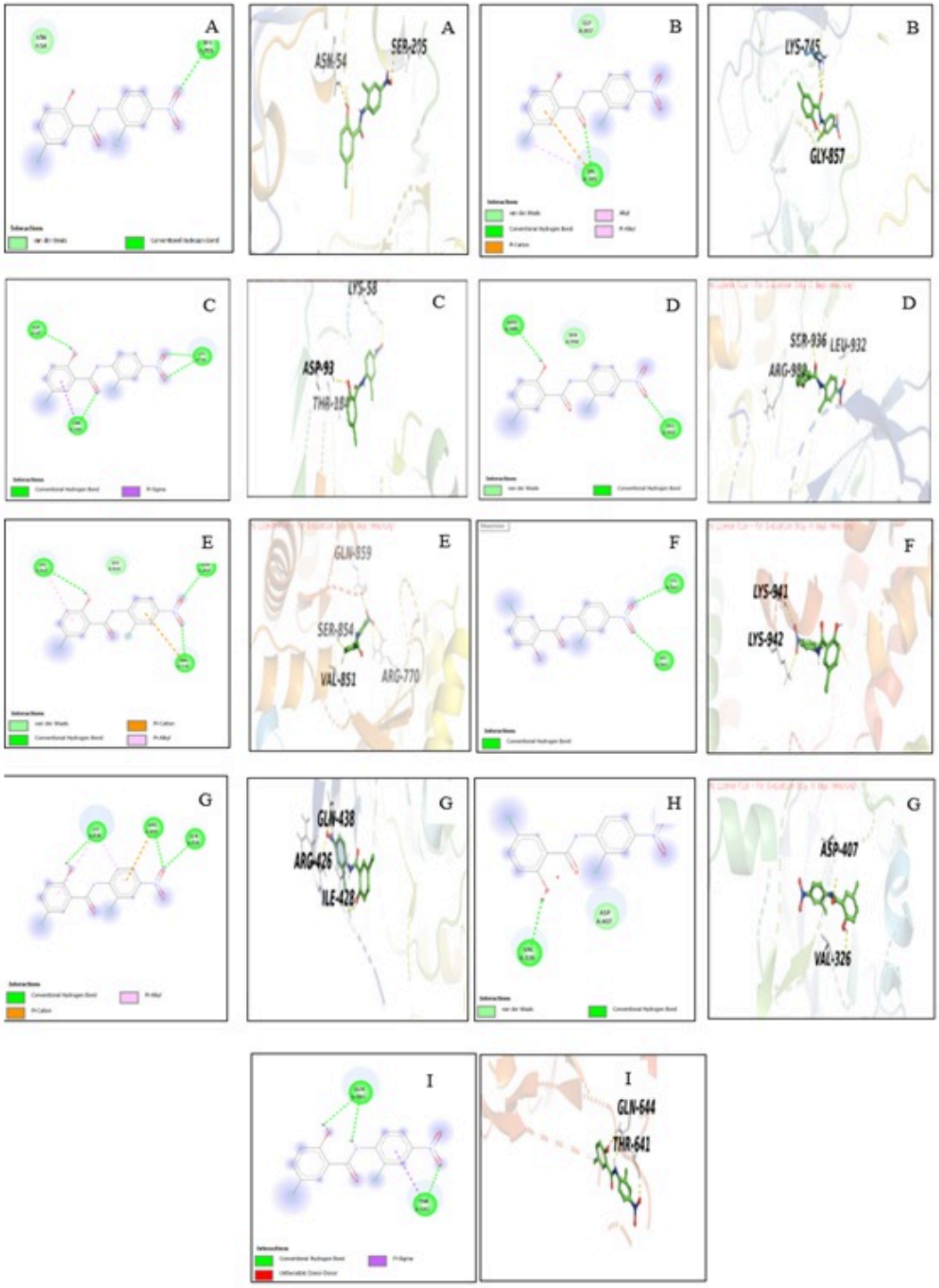

Figure 7

Two-dimensional (2D) and three-dimensional (3D) binding interactions of niclosamide with key hub proteins implicated in HCC.

Niclosamide was docked against the nine core targets identified through network pharmacology and protein–protein interaction analysis, namely AKT1, EGFR, HSP90AA1, JAK2, PIK3R1, PTK2, SRC, and

STAT3. For each target, the left panel illustrates the 2D ligand–protein interaction map, while the right panel depicts the corresponding 3D binding conformation within the active site.

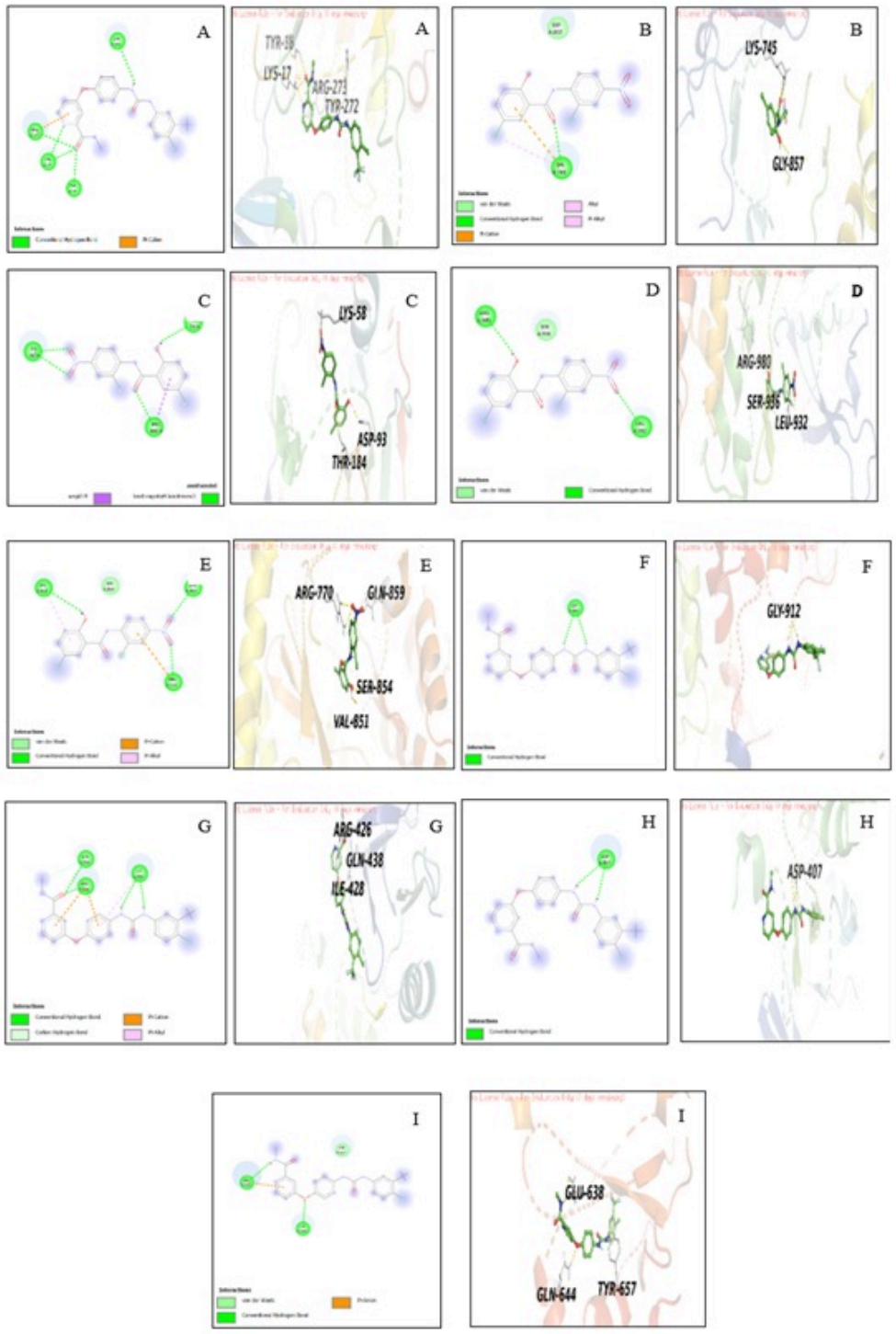

Figure 8

Two-dimensional (2D) and three-dimensional (3D) binding interactions of sorafenib with key hub proteins implicated in HCC.

Sorafenib, the clinically approved first-line systemic therapy for advanced HCC, was docked against the same nine hub targets to serve as a reference control. For each protein, the left panel presents the 2D interaction diagram and the right panel shows the 3D docking pose within the active site.

NIC was docked against the nine core targets identified through network pharmacology and protein–protein interaction analysis, namely AKT1, EGFR, HSP90AA1, JAK2, PIK3R1, PTK2, SRC, and STAT3. For each target, the left panel illustrates the 2D ligand–protein interaction map, while the right panel depicts the corresponding 3D binding conformation within the active site

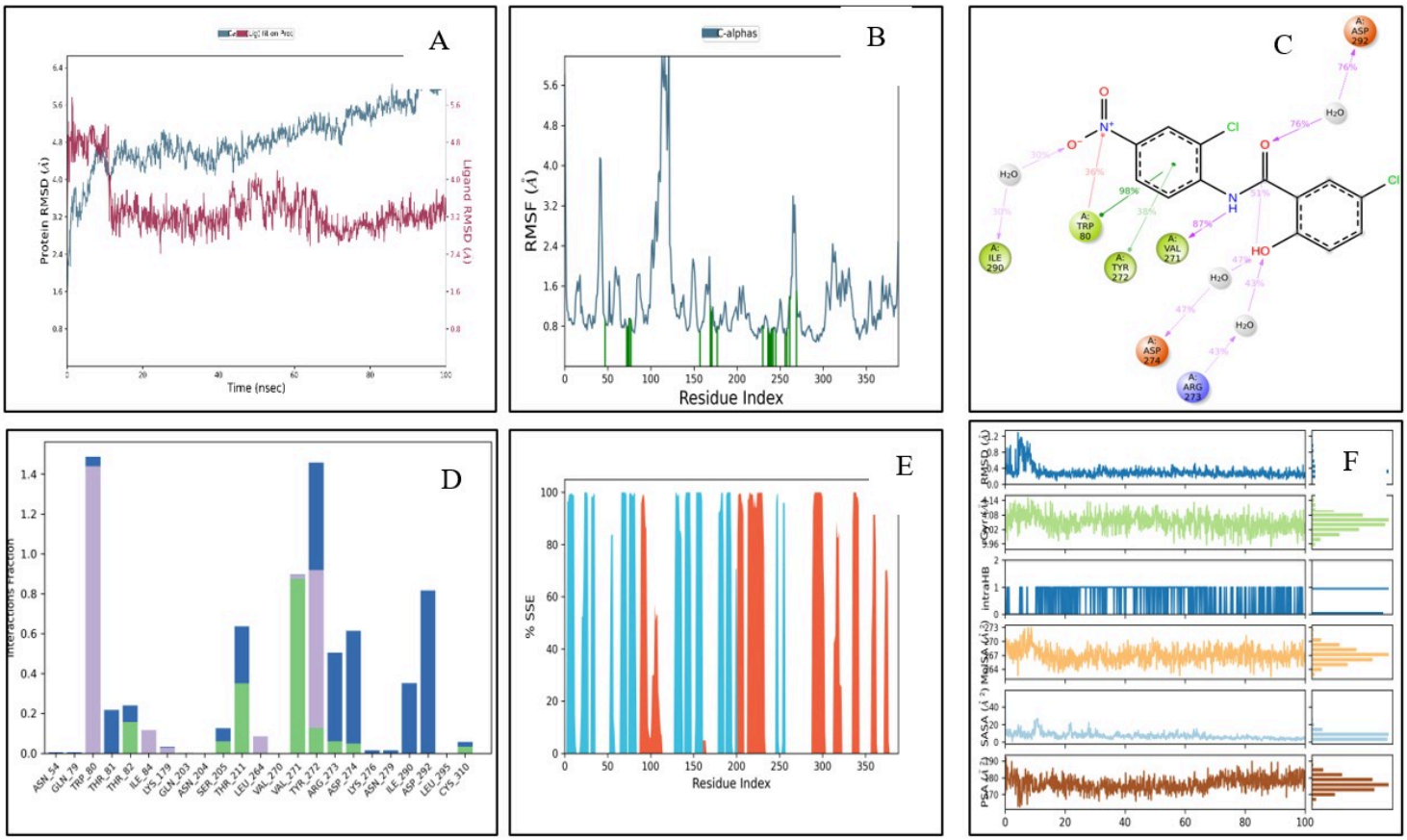

Figure 9

Analysis of the NIC-AKT docking analysis by RMSD, RMSF, Protein-ligand interaction, Secondary structure analysis

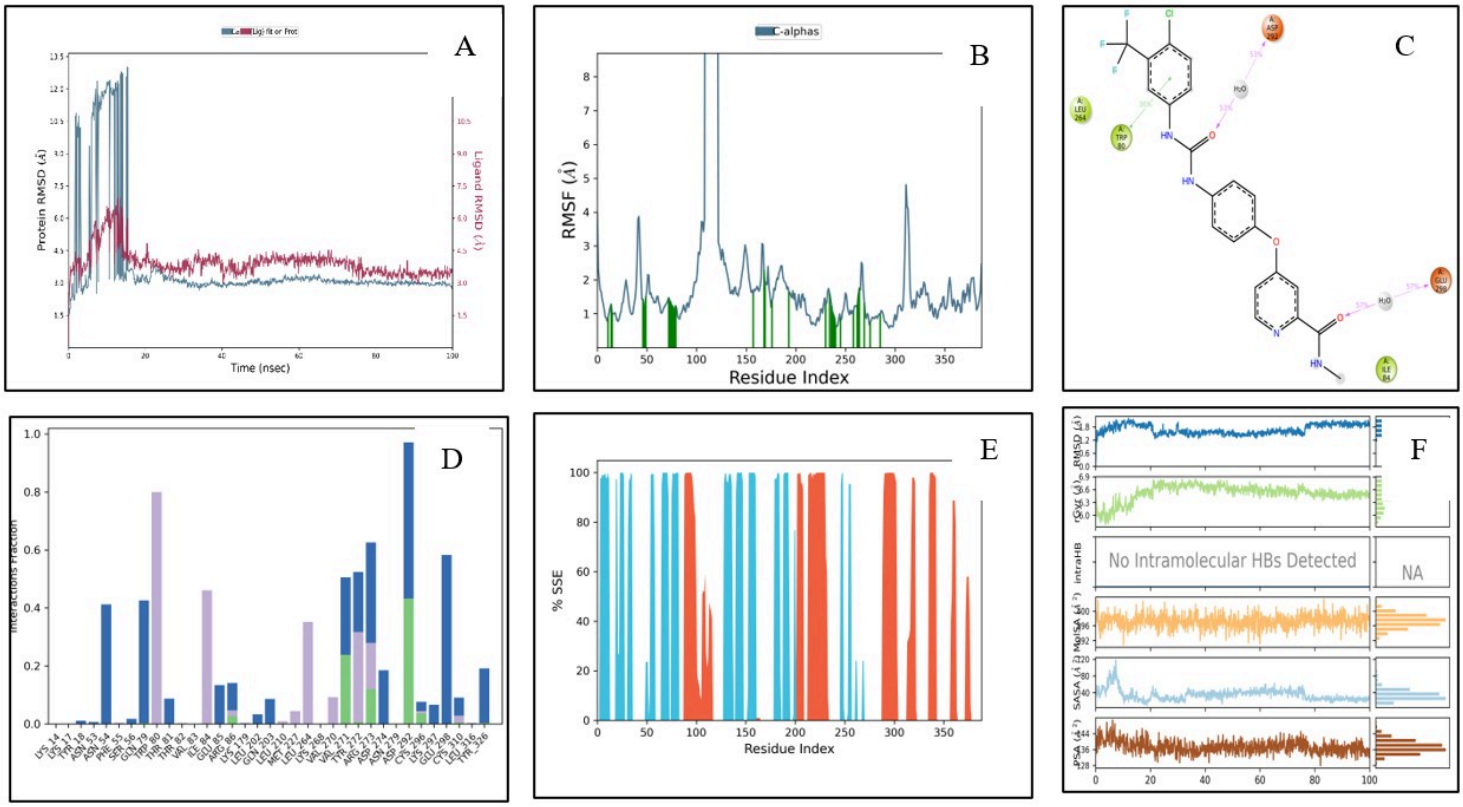

Figure 10

Analysis of the SOR -AKT docking analysis by RMSD, RMSF, ligand protein contacts, Protein-ligand interaction, Secondary structure analysis, ligand properties.

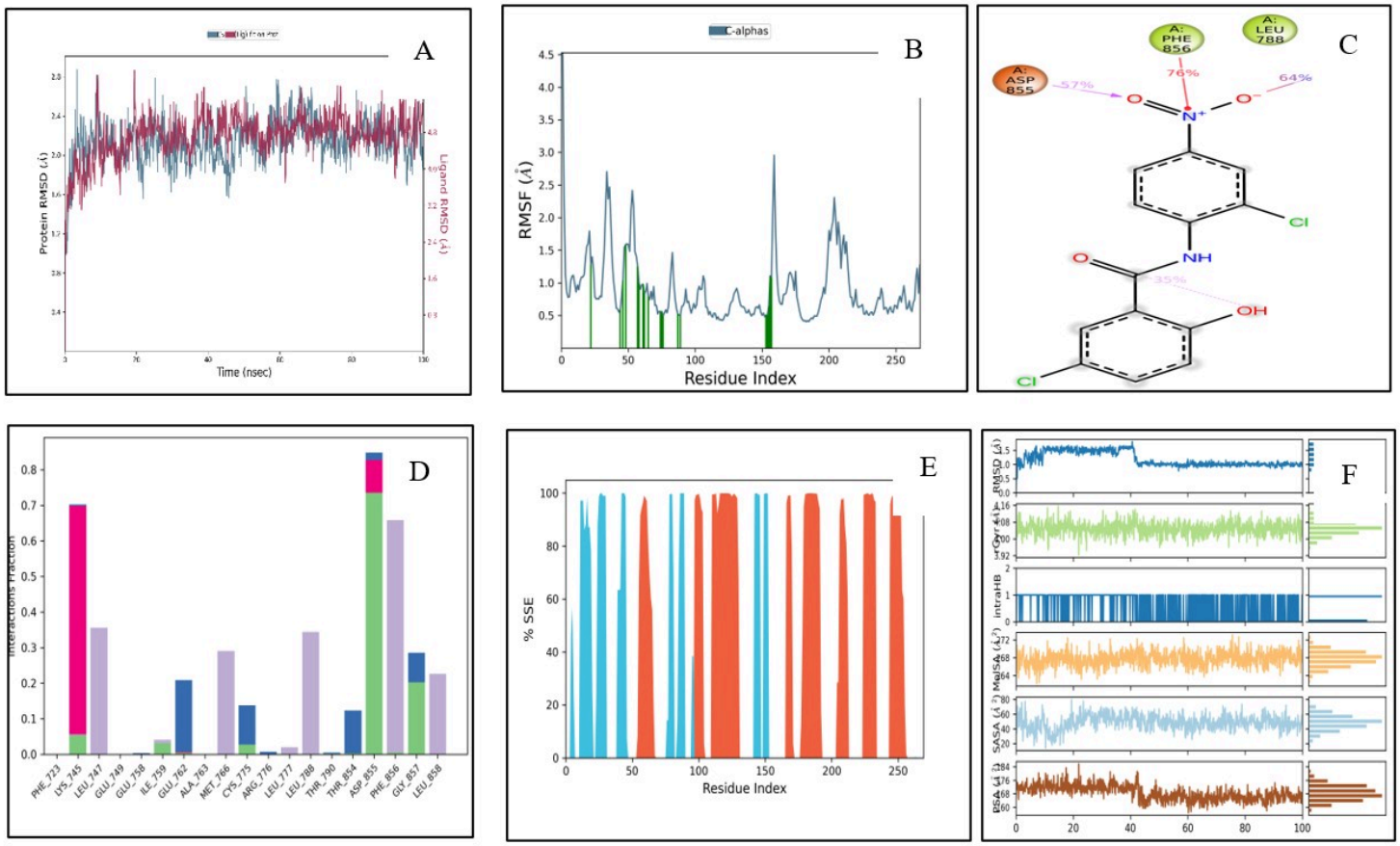

Figure 11

Analysis of the SOR -EGFR docking analysis by RMSD, RMSF, ligand protein contacts, Protein-ligand interaction, Secondary structure analysis, ligand properties.

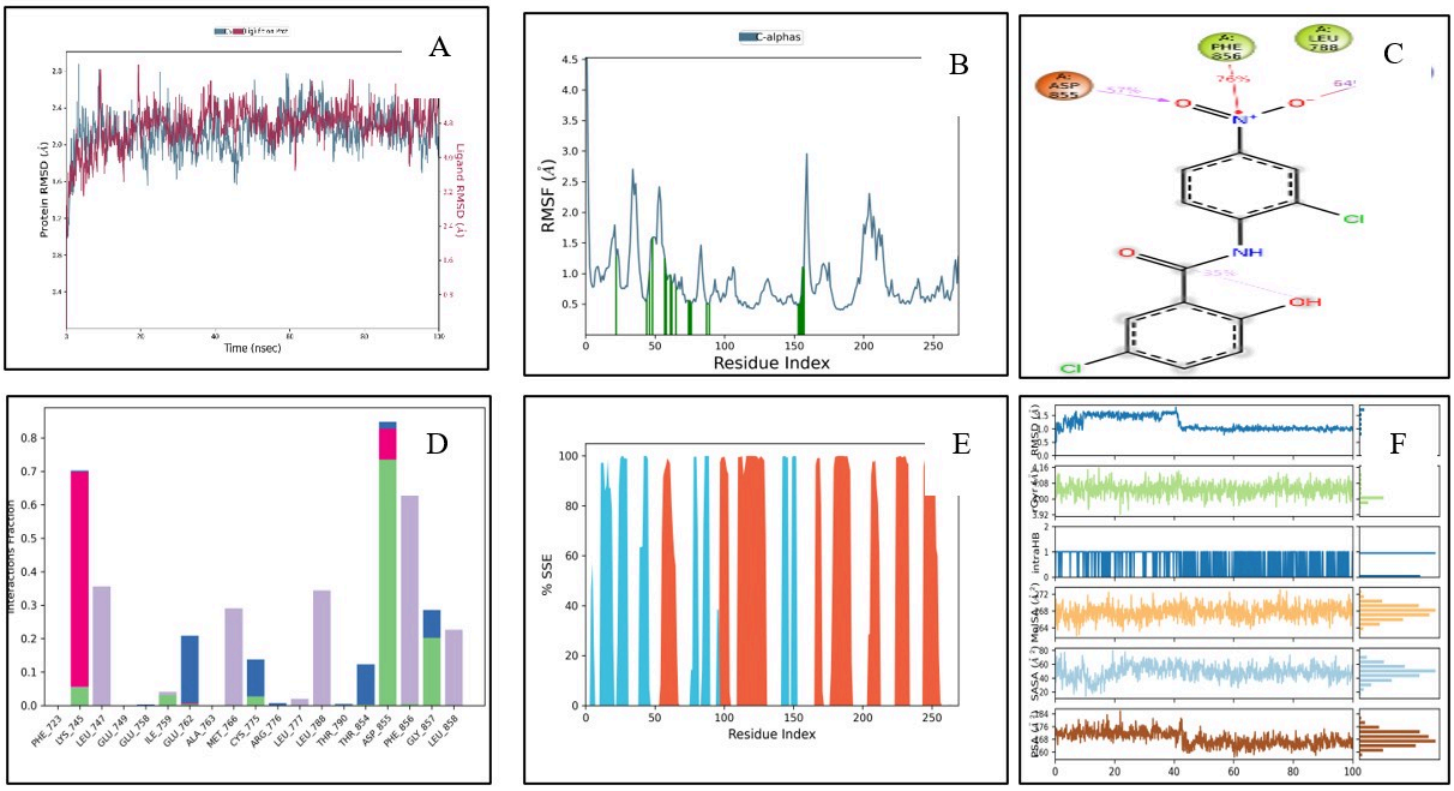

Figure 12

Analysis of the SOR -EGFR docking analysis by RMSD, RMSF, ligand protein contacts, Protein-ligand interaction, Secondary structure analysis, ligand properties.

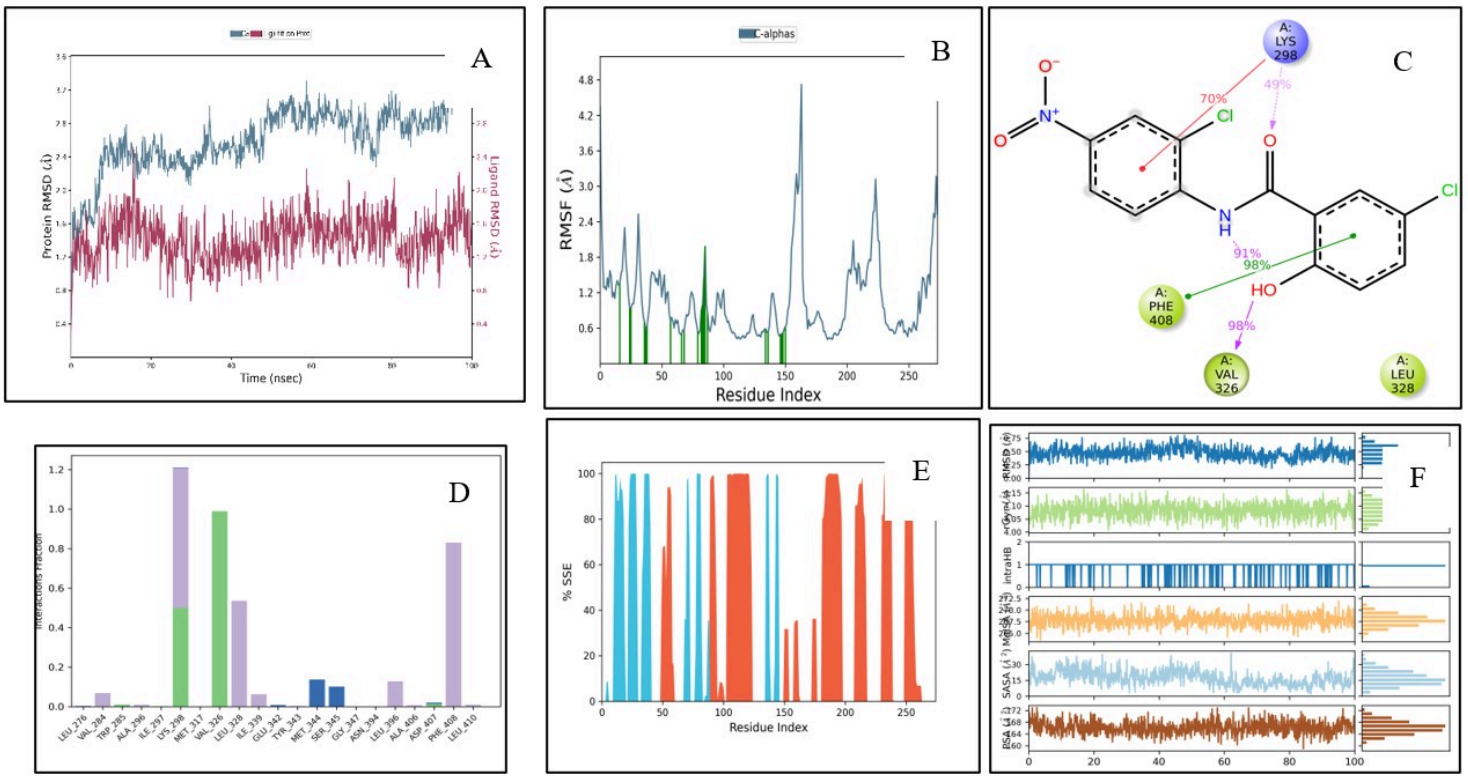

Figure 13

Analysis of the SOR -SRC docking analysis by RMSD, RMSF, ligand protein contacts, Protein-ligand interaction, Secondary structure analysis, ligand properties.

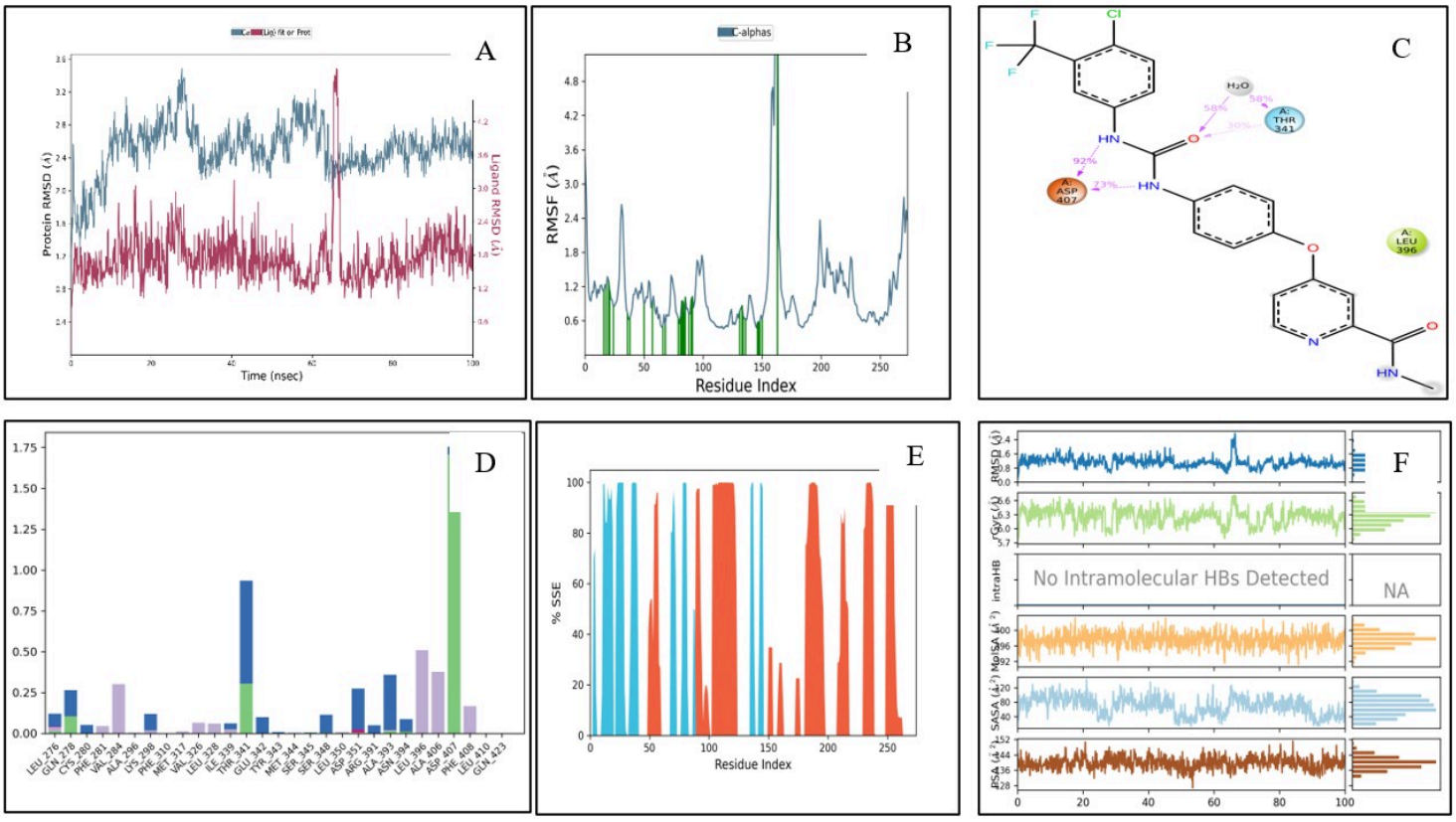

Figure 14

Analysis of the SOR-SRC docking analysis by RMSD, RMSF, ligand protein contacts, Protein-ligand interaction, Secondary structure analysis, ligand properties.